Selective Transfer Machine for Personalized Facial Expression Analysis

Wen-Sheng Chu, Fernando De la Torre, and Jeffrey F. Cohn

Abstract—Automatic facial action unit (AU) and expression detection from videos is a long-standing problem. The problem is challenging in part because classifiers must generalize to previously unknown subjects that differ markedly in behavior and facial morphology (e.g., heavy versus delicate brows, smooth versus deeply etched wrinkles) from those on which the classifiers are trained. While some progress has been achieved through improvements in choices of features and classifiers, the challenge occasioned by individual differences among people remains. Person-specific classifiers would be a possible solution but for a paucity of training data. Sufficient training data for person-specific classifiers typically is unavailable. This paper addresses the problem of how to *personalize* a generic classifier without additional labels from the test subject. We propose a transductive learning method, which we refer to as a Selective Transfer Machine (STM), to personalize a generic classifier by attenuating person-specific mismatches. STM achieves this effect by simultaneously learning a classifier and re-weighting the training samples that are most relevant to the test subject. We compared STM to both generic classifiers and cross-domain learning methods on four benchmarks: CK+ [44], GEMEP-FERA [67], RU-FACS [4] and GFT [57]. STM outperformed generic classifiers in all.

Index Terms—Facial expression analysis, personalization, domain adaptation, transfer learning, support vector machine (SVM)

1 Introduction

Automatic facial AU detection confronts a number of challenges. These include changes in pose, scale, illumination, occlusion, and individual differences in face shape, texture, and behavior. Face shape and texture differ between and within sexes; they differ with ethnic and racial backgrounds, age or developmental level, exposure to the elements, and in the base rates with which they occur. For example, some people smile frequently and broadly, while others smile rarely and only in a controlled manner, counteracting the upward pull of the zygomatic major on the lip corners. These and other sources of variation represent considerable challenges for computer vision. Furthermore, there is the challenge of automatically detecting facial actions that require significant training and expertise in humans [67].

To address these challenges, previous work has focused on identifying optimal feature representations and classifiers. Interested readers may refer to [20], [46], [49], [56] for comprehensive reviews. While improvements have been made, a persistent shortcoming of existing systems is that they fail to generalize well to previously unseen, or new, subjects. One way to cope with this problem is to train and test separate classifiers on each subject (i.e., *person-specific* classifier). Fig. 1a shows a real example of how a simple linear person-specific classifier can separate the positive samples of AU12 (lip corner puller, seen in smiling) from the negative ones. When ample training data are available, a *person-specific classifier* approaches an *ideal classifier*, one that best separates actions for the test subject.

A problem with person-specific classifiers is that a sufficient quantity of training data is usually unavailable. In part for this reason, most approaches use training data from multiple subjects in the hope to compensate for subject biases. However, as shown in Fig. 1b, when a classifier is trained on all training subjects and tested on an unknown subject, its generalizability may disappoint. When a classifier is trained and tested in this manner, we refer to it as a *generic classifier*. Because person-independent classifiers typically are not feasible, generic classifiers are commonly used.

We hypothesize that impaired generalizability occurs in part because of individual differences among subjects. Fig. 2 illustrates this phenomenon on real data in a 3-D eigenspace. One can observe that if the data in Fig. 2a are interpreted as positive and negative classes, they could be very difficult to separate without overfitting. If the data in Fig. 2a are instead interpreted as subjects, the grouping effect becomes clear and echoes our conjecture about individual differences. Individual differences may include sex, skin color and texture, illumination, and other ways in which people and image acquisition effects may vary. Our guiding hypothesis is that the person-specific bias causes standard generic classifiers to perform worse on some subjects than others [28].

To mitigate the influence of individual biases, this paper explores the idea of *personalizing* a generic classifier for facial expression analysis. Given a common observation that a test video usually comes from only a single subject, we assume the test distribution can be approximated by a subset of video frames from training subjects. The problem

- *W.-S. Chu and F.D.la Torre are with the Robotics Institute, Carnegie Mellon University, Pittsburgh, PA 15213. E-mail: wensheng.chu@gmail.com, ftorre@cs.cmu.edu.*
- *J. F. Cohn is with the Robotics Institute, Carnegie Mellon University, and with the Department of Psychology, University of Pittsburgh, Pittsburgh, PA 15260. E-mail: jeffcohn@cs.cmu.edu.*

Manuscript received 3 July 2014; revised 2 Mar. 2016; accepted 17 Mar. 2016. Date of publication 0 . 0000; date of current version 0 . 0000.
Recommended for acceptance by T. Cootes.
For information on obtaining reprints of this article, please send e-mail to: reprints@ieee.org, and reference the Digital Object Identifier below.
Digital Object Identifier no. 10.1109/TPAMI.2016.2547397

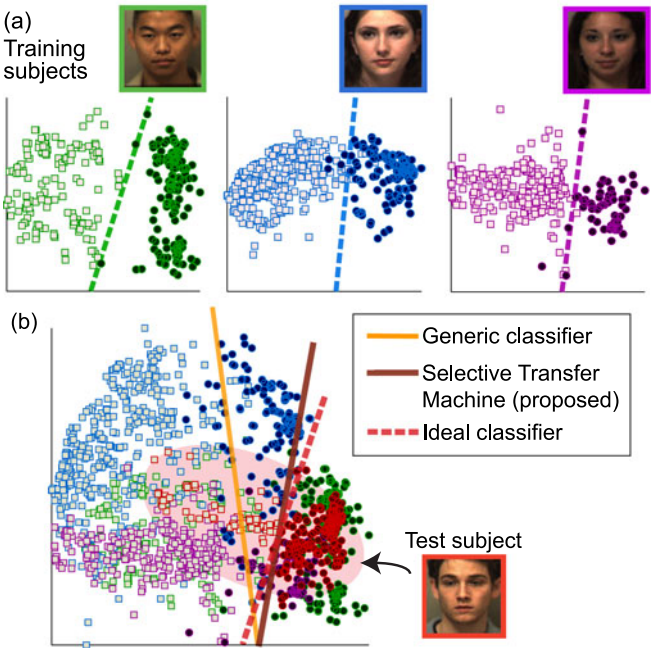

Fig. 1. An illustration of the proposed Selective Transfer Machine (STM): (a) 2D PCA projection of positive (squares) and negative (circles) samples for a given AU (in this case AU 12 or lip-corner raiser) for three subjects. An ideal classifier separates AU 12 nearly perfectly for each subject. (b) A generic classifier trained on all three subjects generalizes poorly to a new person (i.e., test subject) due to individual differences between the 3-subject training set and the new person. STM personalizes a generic classifier and reliably separates an AU for a new subject.

of personalizing a generic classifier is then formulated as training a classifier on selected training samples, while reducing the discrepancy between distributions of selected training samples and test ones. In this way, generic classifiers can adapt to unseen test subjects without test labels. We term this transductive approach a Selective Transfer Machine. The major contributions of this work include:

- Based on both qualitative observations and empirical findings, individual differences attenuate performance of AU detection. To address this problem, we introduce *Selective Transfer Machine (STM)*, an unsupervised personalization approach that reduces mismatch between feature distributions of training and test subjects. We propose an effective and robust procedure to optimize STM in its primal form.
- Considering that many applications afford labeled test data, we introduce a useful extension of STM, termed *L-STM*, to make use of labeled data from the target domain. This extension shows considerable performance improvement in situations where labeled test data are available.
- To evaluate STM, we conduct comprehensive experiments using *within-subject*, *cross-subject*, and *cross-dataset* scenarios on four benchmark datasets. We test STM for both AU detection and detection of holistic expressions.
- For test subjects, some training samples are more instrumental than others. We can identify those training samples using STM. The effectiveness of STM scales as domain size, or the number of training subjects, increases.

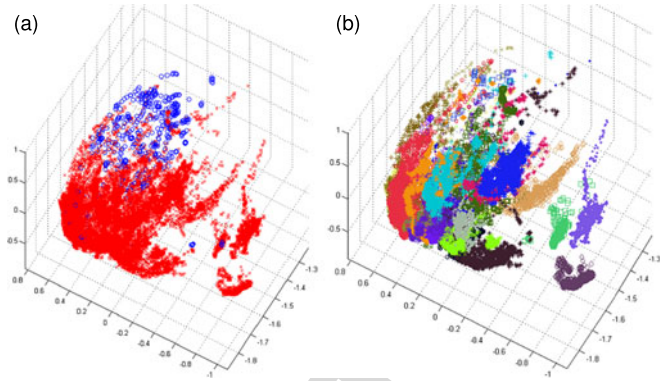

Fig. 2. Visualization of samples from the RU-FACS dataset [4] in 3D eigenspace: colors/markers indicate different (a) positive/negative classes, and (b) subjects (best viewed in color).

This paper is organized as follows. Section 2 reviews related work. Sections 3–5 describe the STM model, optimization algorithm, and theoretical rationale. Section 6 introduces L-STM, an STM extension that utilizes labeled test data. Section 7 considers similarities and differences between STM and related methods. Section 8 evaluates STM and alternatives for AU and holistic expression detection. Section 9 concludes the paper with remarks and future work.

2 Related Work

Our approach lies at the intersection between facial expression analysis and cross-domain adaptation. Below we briefly discuss each in turn.

2.1 Facial Expression Analysis

Automatic facial expression analysis entails at least three steps: Face tracking and registration, feature extraction, and learning classifiers. This section reviews recent advances in each.

Tracking and registration. Tracking and registration of non-rigid facial features is a long-standing problem in computer vision. The goal of tracking is to detect facial landmarks (e.g., eyes) in each frame. For facial landmark detection, Parametrized Appearance Models (PAM) are among the most popular methods. PAM include the Lucas-Kanade method [43], Active Appearance Models (AAM) [18], [47], Constrained Local Models (CLM) [15], and, more recently, Zface [34] and Supervised Descent Method [74]. Once facial landmarks are located, the registration step aims to align the face image to remove 3D rigid head motion, so features can be geometrically normalized. A similarity transformation [20], [61], [86] registers faces with respect to an averaged face. A Delaunay triangulation can be also applied with a backward piecewise affine warping to extract features in areas not explicitly tracked. This two-step registration proves to preserve better shape variation in appearance than by geometric normalization alone.

Feature extraction. With advances in tracking and registration, there has been a renewed emphasis on biologically inspired features and temporal variation. As summarized in Table 1, current approaches to feature extraction may be broadly divided into four types: *geometric*, *appearance*, *dynamic*, and *fusion*. Geometric features contain information about the shape and locations of permanent facial features, such as eyes

TABLE 1
Representative Feature Extraction Methods

Type	Feature	Year	Reference
Geometric	Shape model parametrization	2012	[45]
	Geometry of facial components	2010	[85]
	Landmark locations	2006	[45]
Appearance	Active facial patches	2012	[84]
	SIFT/DAISY	2011	[86]
	Discrete Cosine Transform (DCT)	2011	[27]
	Local Phase Quantization (LPQ)	2011	[35]
	Local Binary Patterns (LBP)	2009	[59], [67]
	Hist. of Oriented Gradient (HOG)	2009	[48]
	Gabor	2006	[4], [41]
	Raw pixels	2000	[37]
Dynamic	Longitudinal expression atlases	2012	[33]
	Gabor motion energy	2010	[73]
	Bag of Temporal Words (BoTW)	2010	[61]
	Volume LBP (LBP-TOP)	2007	[82]
	Optical flow	2005	[32]
Fusion	Multiple feature kernels	2012	[58]

TABLE 2
Representative Classifiers

Type	Classifier	Year	Reference
Static	Deep Networks	2013	[42]
	Support Vector Machine (SVM)	2007	[45]
	AdaBoost	2005	[4]
	Neural Network (NN)	2005	[38]
Temporal	Conditional Random Field (CRF)	2009	[9]
	Gaussian process	2009	[13]
	Dynamic Bayesian Network (DBN)	2007	[65], [70]
	Isomap embedding	2006	[10]
Hybrid	Cascade of Tasks (CoT)	2013	[21]

or nose. Standard approaches rely on detecting fiducial facial points [45], a connected face [61], landmark coordinates [15], or face component shape parameterization [45]. Geometric features have performed well for many but not all AU detection tasks. They have difficulties in detecting subtle expressions and are highly vulnerable to registration error [16].

Appearance features, which often are biologically inspired, afford increased robustness to tracking and registration error. Appearance features represent skin texture and its permutations and have been widely applied to facial expression analysis. Representative methods include SIFT [86], DAISY [86], Gabor jets [4], LBP [35], [84], Bag-of-Words model [60], [61], compositional [77] and others [72]. *Dynamic* features, a newly popular technique, encodes temporal information during the feature extraction stage. Examples include optical flow [32], bag of temporal words [62], volume LBP/LPQ [82], Gabor motion energy [73], and others. *Fusion* approaches incorporate multiple features, e.g., Multiple Kernel Learning (MKL) [58], and have yet to prove superior to other approaches [67].

Classifiers. Two main trends have been pursued when designing classifiers for facial expression analysis, as summarized in Table 2. One trend, *static modeling*, typically tackles the problem as discriminative classification and evaluates each frame independently. Representative approaches include Neural Network [38], Adaboost [4], SVMs [45], [61], [83], and Deep Networks [42]. Due to lack of temporal consistency, static models tend to produce non-smooth results. To address this issue, *temporal modeling*, the other trend, captures the temporal transition between contiguous frames. For instance, Dynamic Bayesian Network (DBN) with appearance features [65] was proposed to model AU co-occurrence. Other variants of DBN include Hidden Markov Models [59] and Conditional Random Fields (CRF) [9], [68]. As an alternative, Simon et al. [61] proposed a structural-output SVM that detects AUs as temporal segments. To model relations between segments, Rudovic et al. [52] considered ordinal information in CRF. More recently, Ding et al. [21] proposed a hybrid approach that integrates frame-based, segment-based, and transition-based tasks in a sequential order. Interested readers are referred to [20], [46], [49], [56], [67] for more complete surveys.

Common to all these approaches is the assumption that training and test data are drawn from the same distribution. However, as Fig. 2 shows, they could suffer from individual differences, causing poor generalizability to an unseen subject. STM makes no such assumption. Instead, it seeks a personalized classifier by re-weighting training samples according to their distribution mismatch with test samples. Several studies merged into this direction could be found in [55], [78], [79], [80].

2.2 Cross-Domain Adaptation

Our approach is motivated by an increasing concern about dataset shift in the object detection literature. In real-world data, labels of interest could occur infrequently and features vary markedly between and within datasets. These factors contribute to significant biases in object categorization [66]. Saenko et al. [40], [54] proposed to reduce the discrepancy between features by learning metric transformation. Aytar and Zisserman [2] regularized the training of a new object class by transferring pre-learned models. Chattopadhyay et al. [12] proposed to learn a combination of source classifiers that matches the target labels. Because these techniques use a supervised approach in which one or more labeled instances are required from the target domain, they are ill-suited to new domains or subjects for which no prior knowledge is available. In contrast, our approach is unsupervised and thus better geared to the generalization to new domains or subjects.

Closer to our approach is a special case in unsupervised domain adaptation known as *covariate shift* [63]. In covariate shift, train and test domains follow different distributions but the label distributions remain the same.

On the other hand, Dudík et al. [24] infer the re-sampling weights through maximum entropy density estimation without target labels. Maximum Mean Discrepancy (MMD) [5] measures the discrepancy between two different distributions in terms of expectations of empirical samples. Without estimating densities, Transductive SVM (T-SVM) [36] simultaneously learns a decision boundary and maximizes the margin in the presence of unlabeled patterns. Domain adaptation SVM [6] extends T-SVM by progressively adjusting the discriminant function toward the target domain. SVM-KNN [81] labels a single query using an SVM trained on its k neighborhood of the training data. Each of these methods uses either all or a portion of the training data. STM learns to re-weight training instances, which reduces the influence of irrelevant data.

Considering distribution mismatch, Kernel Mean Matching (KMM) [31] directly infers re-sampling weights by

matching training and test distributions. Following this idea, Yamada et al. [75] estimated relative importance weights and learned from re-weighted training samples for 3D human pose estimation. See [50] for further review. These methods take a two-step approach that first estimates the sampling weights and then trains a re-weighted classifier or regressor. In contrast, STM jointly optimizes both the sampling weights and the classifier parameters and hence preserves the discriminant property of the new decision boundary.

3 Selective Transfer Machine (STM)

This section describes the proposed Selective Transfer Machine (STM) for personalizing a generic classifier. Unlike previous cross-domain methods [2], [22], [39], [76], STM requires no labels from a test subject. For classification purpose, we model STM with a Support Vector Machine (SVM) due to its popularity for AU detection [15], [35], [61].

Problem formulation. Recent research and applications in automatic facial expression analysis consider video data, which provide a wide sampling of facial appearance changes. We assume the distribution of a subject's appearance can be estimated by certain video frames. Based on this assumption, the main idea of STM is to re-weight training samples (i.e., frames) to form a distribution that approximates the test distribution. Classifiers trained on the re-weighted training samples are likely to generalize to the test subject.

Denote the training set as $\mathcal{D}^{\text{tr}}=\{\mathbf{x}_i, y_i\}_{i=1}^{n_{\text{tr}}},\ y_i\in\{+1,-1\}$ (see notation[1]). For notational simplicity, we stack 1 in each data vector $\mathbf{x}_i$ to compensate for the offset, i.e., $\mathbf{x}_i\in\mathbb{R}^{d+1}$. We formulate STM as minimizing the objective:

$$g(f,\mathbf{s}) = \min_{f,\mathbf{s}} R_f(\mathcal{D}^{\text{tr}},\mathbf{s}) + \lambda\Omega_{\mathbf{s}}(\mathbf{X}^{\text{tr}},\mathbf{X}^{\text{te}}), \tag{1}$$

where $R_f(\mathcal{D}^{\text{tr}},\mathbf{s})$ is the SVM empirical risk defined on the decision function f, and training set $\mathcal{D}^{\text{tr}}$ with each instance weighted by selection coefficients $\mathbf{s}\in\mathbb{R}^{n_{\text{tr}}}$. Each entry s_i corresponds to a positive weight for a training sample $\mathbf{x}_i$. $\Omega_{\mathbf{s}}(\mathbf{X}^{\text{tr}},\mathbf{X}^{\text{te}})$ measures training and test distribution mismatch as a function of $\mathbf{s}$. The lower the value of $\Omega_{\mathbf{s}}$ is, the closer the training and the test distributions are. $\lambda>0$ is a tradeoff between the risk and the distribution mismatch. The goal of STM is to jointly optimize the decision function f as well as the selective coefficient $\mathbf{s}$, such that the resulting classifier can alleviate person-specific biases.

Penalized SVM. The first term in STM, $R_f(\mathcal{D}^{\text{tr}},\mathbf{s})$, is the empirical risk of a penalized SVM, where each training instance is weighted by its relevance to the test data. In the following, we denote $\mathbf{X}\equiv\mathbf{X}^{\text{tr}}$ for notational simplicity unless further referred. The linear penalized SVM has the target decision function in the form $f(\mathbf{x})=\mathbf{w}^\top\mathbf{x}$ and minimizes:

$$R_{\mathbf{w}}(\mathcal{D}^{\text{tr}},\mathbf{s}) = \frac{1}{2}\|\mathbf{w}\|^2 + C\sum_{i=1}^{n_{\text{tr}}} s_i L^p(y_i,\mathbf{w}^\top\mathbf{x}_i), \tag{2}$$

where $L^p(y,\cdot)=\max(0,1-y\cdot)^p$ ($p=1$ stands for hinge loss and $p=2$ for quadratic loss). In general, L could be any loss function. The unconstrained linear SVM in (2) can be extended to a nonlinear version by introducing a kernel matrix $\mathbf{K}_{ij}:=k(\mathbf{x}_i,\mathbf{x}_j)$, which corresponds to a kernel function k induced from a nonlinear feature mapping $\varphi(\cdot)$. Using the representer theorem [11], the nonlinear decision function can be represented $f(\mathbf{x})=\sum_{i=1}^{n_{\text{tr}}}\beta_i k(\mathbf{x}_i,\mathbf{x})$, yielding the nonlinear penalized SVM:

$$R_{\boldsymbol{\beta}}(\mathcal{D}^{\text{tr}},\mathbf{s}) = \frac{1}{2}\boldsymbol{\beta}^\top\mathbf{K}\boldsymbol{\beta} + C\sum_{i=1}^{n_{\text{tr}}} s_i L^p(y_i,\mathbf{k}_i^\top\boldsymbol{\beta}), \tag{3}$$

where $\boldsymbol{\beta}\in\mathbb{R}^{n_{\text{tr}}}$ is the expansion coefficient and $\mathbf{k}_i$ is the ith column of $\mathbf{K}$. Unlike most standard solvers, we train the penalized SVM in the primal due to its simplicity and efficiency. Through the unconstrained primal problems, we apply Newton's method with quadratic convergence [11]. Details are given in Section 4.

Distribution mismatch. The second term in STM, $\Omega_{\mathbf{s}}(\mathbf{X}^{\text{tr}},\mathbf{X}^{\text{te}})$, imitates domain mismatch and aims to find a re-weighting function that minimizes the discrepancy between the training and the test distributions. In previous cross-domain learning methods, the re-weighting function may be computed by separately estimating the densities and then the weights (e.g., [64]). However, this strategy could be prone to error while taking the ratio of estimated densities [64].

To estimate the re-weighting function, here we adopt the Kernel Mean Matching (KMM) [31] method, which aims to reduce the distance of empirical means between the training and the test distributions in the Reproducing Kernel Hilbert Space $\mathcal{H}$. KMM computes the instance re-weighting s_i that minimizes:

$$\Omega_{\mathbf{s}}(\mathbf{X}^{\text{tr}},\mathbf{X}^{\text{te}}) = \left\| \frac{1}{n_{\text{tr}}}\sum_{i=1}^{n_{\text{tr}}} s_i\varphi(\mathbf{x}_i^{\text{tr}}) - \frac{1}{n_{\text{te}}}\sum_{j=1}^{n_{\text{te}}}\varphi(\mathbf{x}_j^{\text{te}}) \right\|_{\mathcal{H}}^2. \tag{4}$$

Let $\kappa_i:=\frac{n_{\text{tr}}}{n_{\text{te}}}\sum_{j=1}^{n_{\text{te}}} k(\mathbf{x}_i^{\text{tr}},\mathbf{x}_j^{\text{te}})$, $i=1,\ldots,n_{\text{tr}}$, capture the closeness between a training sample and each test sample, solving $\mathbf{s}$ in (4) can be rewritten as a quadratic programming (QP):

$$\begin{aligned} \min_{\mathbf{s}}\ & \frac{1}{2}\mathbf{s}^\top\mathbf{K}\mathbf{s} - \boldsymbol{\kappa}^\top\mathbf{s}, \\ \text{s.t.}\ & s_i\in[0,B], \left|\sum_{i=1}^{n_{\text{tr}}} s_i - n_{\text{tr}}\right| \le n_{\text{tr}}\epsilon, \end{aligned} \tag{5}$$

where B defines a scope that bounds discrepancy between probability distributions P_{tr} and P_{te} ($B=1{,}000$ in our case). For $B\to 1$, one obtains an unweighted solution where all $s_i=1$. The second constraint ensures the weighted samples to be close to a probability distribution [31]. Observe in (5) that a larger κ_i leads to a larger s_i to minimize the objective. This matches our intuition to put higher selection weights on the training samples that are more likely to resemble the test distribution.

A major benefit from KMM is a direct importance estimation without estimating training and test densities. Compared to existing approaches, with proper tuning of kernel bandwidth, KMM shows the lowest importance estimation error, and robustness to input dimension and the number of training samples [64]. Fig. 3 illustrates its effect on a synthetic data. As shown, KMM can estimate the ideal fitting well, while standard Ordinary Least Square (OLS) and

1. Bold capital letters denote a matrix $\mathbf{X}$; bold lower-case letters denote a column vector $\mathbf{x}$. $\mathbf{x}_i$ represents the ith column of the matrix $\mathbf{X}$. All non-bold letters represent scalars. x_j denotes the scalar in the jth element of $\mathbf{x}$. $I_n\in\mathbb{R}^{n\times n}$ is an identity matrix.

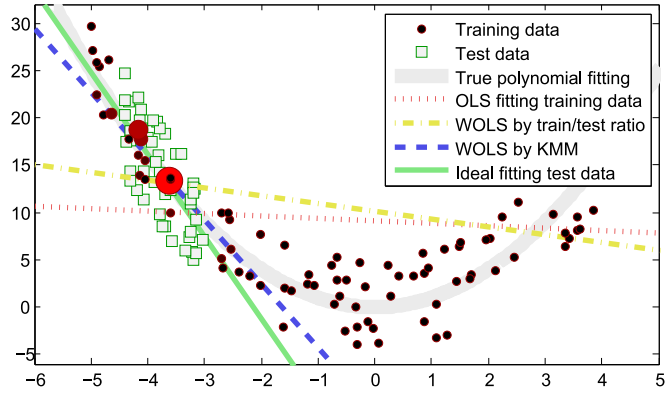

Fig. 3. Fitting a line to a quadratic function using KMM and other re-weighting methods. The larger size (more red) of training data, the more weight KMM adopted. As can be observed, KMM puts higher weights in the training samples closer to the test ones. Compared to standard OLS or WOLS, KMM leads to better approximation for the test data.

Weighted OLS (WOLS) with training/test ratio lead to sub-optimal prediction.

4 Optimization for STM

To solve Eq. (1), we adopt Alternate Convex Search [26] that alternates between solving the decision function f and the selection coefficient $\mathbf{s}$. Note that the objective in (1) is biconvex: Convex in f when $\mathbf{s}$ is fixed (f is quadratic and L^p is convex), and convex in $\mathbf{s}$ when f is fixed (since $\mathbf{K}\succeq 0$). Under these conditions, the alternate optimization approach is guaranteed to monotonically decrease the objective function. Because the function is bounded below, it will converge to a critical point. Algorithm 1 summarizes the STM algorithm. Once the optimization is done, f is applied to perform the inference for test images. Below we detail the two steps in the alternate algorithm.

Minimizing over $\mathbf{s}$. Denote the training losses as $\ell_i^p := L^p(y_i, f(\mathbf{x}_i))$, $i=1,\ldots,n_{\text{tr}}$. The optimization over $\mathbf{s}$ can be rewritten into the following QP:

$$\begin{aligned} \min_{\mathbf{s}} \quad & \frac{1}{2}\mathbf{s}^\top \mathbf{K}\mathbf{s} + (\frac{C}{\lambda}\boldsymbol{\ell}^p - \boldsymbol{\kappa})^\top \mathbf{s} \\ \text{s.t.} \quad & 0 \le s_i \le B, n_{\text{tr}}(1-\epsilon) \le \sum_{i=1}^{n_{\text{tr}}} s_i \le n_{\text{tr}}(1+\epsilon). \end{aligned} \tag{6}$$

Since $\mathbf{K}\succeq 0$ by definition, (6) has only one global optimum. To make the algorithm numerically stable, we add a ridge σ on the diagonal so that $\mathbf{K} \succeq \sigma \mathbf{I}_{n_{\text{tr}}}$ ($\sigma = 10^{-8}$ in our case).

Note that the procedure here is different from the original KMM in terms of *weight refinement*: In each iteration $\mathbf{s}$ will be refined through the training loss $\boldsymbol{\ell}^p$ from the penalized SVM. This effect can be observed from minimizing the second term in (6): Larger $\boldsymbol{\ell}^p$ leads to smaller $\mathbf{s}$ to keep the objective small. This effectively reduces the selection weights of misclassified training samples. On the contrary, KMM uses no label information and thus is incapable of refining importance weights. Introducing training losses helps preserve the discriminant property of the new decision boundary and hence leads to a more robust personalized classifier. From this perspective, KMM can be treated as a special case as the first iteration in STM.

Algorithm 1. Selective Transfer Machine

Input: $\mathbf{X}^{\text{tr}}$, $\mathbf{X}^{\text{te}}$, parameters C, λ
Output: Inferred test labels $\mathbf{y}^\star$ for test data
1 Initialize training loss $\boldsymbol{\ell}^p \leftarrow \mathbf{0}$;
2 **while** *not converged* **do**
3 Update the instance-wise re-weighting $\mathbf{s}$ by solving the QP in (6);
4 Update the decision function f and training loss $\boldsymbol{\ell}^p$ by solving the penalized SVM in (2) or (3);
5 Infer test labels by $\mathbf{y}^\star \leftarrow f(\mathbf{X}^{\text{te}})$

Fig. 5 illustrates the iterative effect of personalizing a generic classifier on a synthetic example. In `it#1`, the hyperplane estimated by KMM is unreliable due to its unsupervised nature. On the other hand, STM simultaneously considers the SVM loss and the similarity between training and test samples, and thus encourages the associated training samples with small training loss to be weighted more. As can be observed, as the iterations proceed, the STM separation hyperplane moves toward the ideal hyperplane for the target data.

Minimizing over f. Let sv indicate the index set of support vectors, and n_{sv} the number of support vectors. In the case training loss ℓ^2 being quadratic, the gradient and the Hessian of the linear penalized SVM in (2) can be written as:

$$\nabla_{\mathbf{w}} = \mathbf{w} + 2C\mathbf{X}\mathbf{S}\mathrm{I}^0(\mathbf{X}^\top\mathbf{w} - \mathbf{y}), \tag{7}$$

$$\mathbf{H}_{\mathbf{w}} = I_d + 2C\mathbf{X}\mathbf{S}\mathrm{I}^0\mathbf{X}^\top, \tag{8}$$

where $\mathbf{S} = \text{diag}(\mathbf{s}) \in \mathbb{R}^{n_{\text{tr}}\times n_{\text{tr}}}$ denotes the re-weighting matrix, $\mathbf{y} \in \mathbb{R}^{n_{\text{tr}}}$ the label vector, and $\mathbf{I}^0 \in \mathbb{R}^{n_{\text{tr}}\times n_{\text{tr}}}$ the proximity identity matrix with the first n_{sv} diagonal elements being 1 and the rest being 0. Similarly, the gradient with respect to the expansion coefficient $\boldsymbol{\beta}$ in (3) can be derived as:

$$\nabla_{\boldsymbol{\beta}} = \mathbf{K}\boldsymbol{\beta} + 2C\mathbf{K}\mathbf{S}\mathrm{I}^0(\mathbf{K}\boldsymbol{\beta} - \mathbf{y}), \tag{9}$$

$$\mathbf{H}_{\boldsymbol{\beta}} = \mathbf{K} + 2C\mathbf{K}\mathbf{S}\mathrm{I}^0\mathbf{K}. \tag{10}$$

Given the gradients and the Hessians, the penalized SVM can be optimized in the primal using standard Newton's method or conjugate gradient.

Differentiable huber loss. The L^1 (hinge) loss in standard SVMs are not differentiable, hampering its gradient and Hessian to be explicitly expressed and computed. Instead, we use the Huber loss [11] as a differentiable surrogate, i.e., $L^1(y_i, f(\mathbf{x}_i)) \approx L_H(y_i \text{sign}(f(\mathbf{x}_i)))$. Note that any differential convex loss, e.g., logistic loss and exponential loss, can be directly incorporated. The Huber loss is defined as:

$$L_H(a) = \begin{cases} 0 & \text{if} a > 1+h, \\ \frac{(1+h-a)^2}{4h} & \text{if } |1-a| \le h, \\ 1-a & \text{otherwise}, \end{cases} \tag{11}$$

where h is a parameter of choice. Fig. 4 shows the influnce of h in comparison to the L^1 and L^2 loss. As can be observed, L_H approaches the hinge loss when $h \to 0$. As indicated in [11], there is no clear reason to prefer the hinge loss because replacing the hinge loss with Huber loss does not influence much the results. With the differentiable Huber loss, the gradient and Hessian with Huber loss for the penalized linear SVM can be obtained:

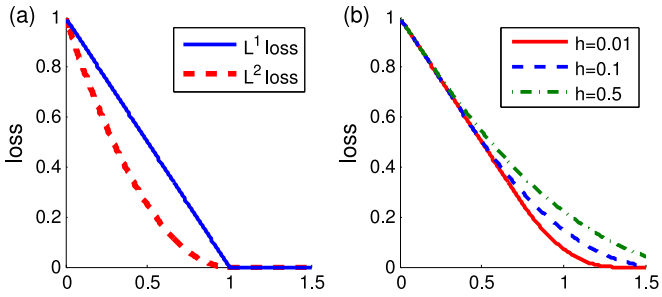

Fig. 4. Loss functions: (a) L^1 and L^2 loss, and (b) Huber loss.

$$\nabla_{\mathbf{w}} = \mathbf{w} + \frac{C}{2h}\mathbf{X}\mathbf{S}\mathbf{I}^0\left[\mathbf{X}^\top\mathbf{w} - (1+h)\mathbf{y}\right] - C\mathbf{X}\mathbf{S}\mathbf{I}^1\mathbf{y}, \tag{12}$$

$$\mathbf{H}_{\mathbf{w}} = \mathbf{I}_d + \frac{C}{2h}\mathbf{X}\mathbf{S}\mathbf{I}^0\mathbf{X}^\top, \tag{13}$$

and for the penalized nonlinear SVM:

$$\nabla_{\boldsymbol{\beta}} = \mathbf{K}\boldsymbol{\beta} + \frac{C}{2h}\mathbf{K}\mathbf{S}\mathbf{I}^0[\mathbf{K}\boldsymbol{\beta} - (1+h)\mathbf{y}] - \mathbf{K}\mathbf{I}^1\mathbf{y}, \tag{14}$$

$$\mathbf{H}_{\boldsymbol{\beta}} = \mathbf{K} + \frac{C}{2h}\mathbf{K}\mathbf{S}\mathbf{I}^0\mathbf{K}, \tag{15}$$

where $\mathbf{I}^1 \in \mathbb{R}^{n_{\text{tr}} \times n_{\text{tr}}}$ denotes the proximity identity matrix with the first n_{sv} diagonal elements being 0, followed by n_ℓ (the number of points in the linear part of the Huber loss) elements of ones. With the derived gradients and Hessians, we optimize for f using standard Newton method.

5 Theoretical Rationale

This section analyzes two important properties of STM, *biconvexity* and *boundedness*, based on the techniques developed for biconvex optimization [30]. Then we justify the convergence of the Alternate Convex Search algorithm, which we used for solving STM, in terms of both objective value and optimization variables.

5.1 Properties of STM

We start by showing that STM is a biconvex problem.

Property 1. *(Bi-convexity) Selective Transfer Machine in (1) is a* biconvex optimization problem.

Proof. Denote the decision variable of f as $\mathbf{w} \in W \subseteq \mathbb{R}^d$ and the selection coefficient $\mathbf{s} \in S \subseteq \mathbb{R}^{n_{\text{tr}}}$, where W and S are two non-empty convex sets. Let $Z \subseteq W \times S$ be the solution set on $W \times S$; $Z_{\mathbf{w}}$ and $Z_{\mathbf{s}}$ be the subsets when $\mathbf{w}$ and $\mathbf{s}$ are given respectively. Because $Z_{\mathbf{s}}$ is convex for every $\mathbf{w} \in W$ ($\mathbf{w}$ and L^p are convex; $s_i \in [0, B]$ are non-negative) and $Z_{\mathbf{w}}$ is convex for every $\mathbf{s} \in S$ ($\Omega_{\mathbf{s}}$ is QP and $\mathbf{K} \succeq 0$), the solution set Z is a *biconvex set*. Hence STM can be rewritten in the standard form of *biconvex optimization problem* [1]: $\min_{\mathbf{w},\mathbf{s}}\{g(\mathbf{w},\mathbf{s}) : (\mathbf{w},\mathbf{s}) \in Z\}$. □

Property 2. *(Boundedness) The STM optimization problem in Problem (1) is bounded from below.*

Proof. The boundedness can be observed from two aspects: (1) R_f is bounded due to the quadratic term in f and non-negative $\mathbf{s}$ and L^p. (2) Ω_s is bounded since $\mathbf{K}$ is positive semi-definite. □

Following the same proof line, the above properties can be also shown for nonlinear STM defined with Eq. (3).

5.2 Algorithm

The following analysis mimics directly Section 4 in [30]. We present the key steps for proving the convergence and refer to more details on this style of proof in [30].

Alternate convex search. To solve the biconvex STM problem, one approach is to exploit its convex substructure. We used the Alternate Convex Search (ACS) algorithm [71], a special case of *Block-Relaxation Methods*, by alternately solving the convex subproblems. For explanation convenience, we recall the ACS algorithm in Algorithm 2.

Denote $\mathbf{z} = (\mathbf{w}, \mathbf{s})$ as the solution variable. As mentioned in Section 4, STM can be seen as initializing $\mathbf{s}_0$ using KMM or a uniform vector, and then solving the classifier $\mathbf{w}_1$ as an unweighed SVM. As will be discussed below and in Section 8.5, the permutation order does not influence the convergence. For Step 4, there are several ways to determine the stopping criterion. We used the relative decrease of $\mathbf{z}$ compared to the last iteration. Below we discuss the convergence properties in terms of objective value (i.e., the difference between $g(\mathbf{z}_t)$ and $g(\mathbf{z}_{t-1})$ of two consecutive iterations t and $t-1$), and the variables (i.e., the difference between $\mathbf{z}_t$ and $\mathbf{z}_{t-1}$).

Convergence. Recall that W and S are two non-empty sets, and $Z \subseteq W \times S$ is a biconvex set on $W \times S$. We firstly show

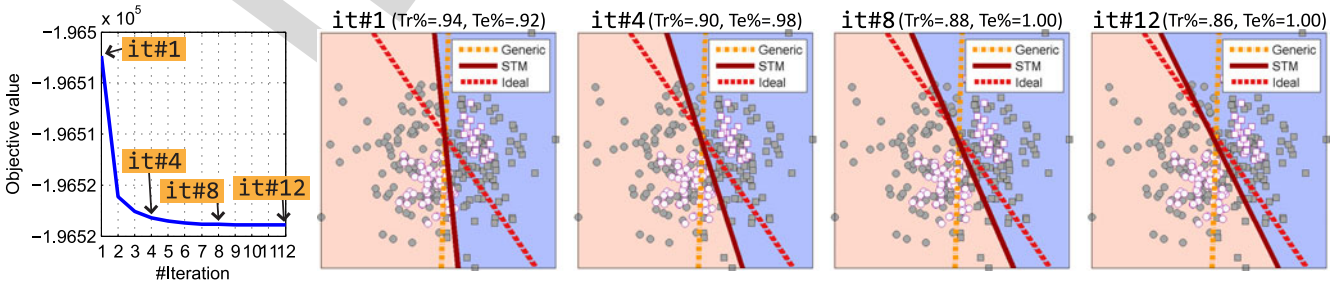

Fig. 5. Comparisons of a generic SVM, a personalized STM, and an ideal classifier for synthetic data. The left-most figure shows the convergence curve of the objective value. Figures `it#1,4,8,12` with training/test accuracy (Tr% and Te%) show the corresponding hyperplanes at each iteration. Grey (shaded) dots denote training samples, and white (unshaded) dots denote test samples. Circles and squares denote two different classes. Note that `it#1` indicates the results of KMM [31]. STM improves separation relative to the generic SVM as early as the 1st iteration and converges toward the ideal hyperplane by the 12th iteration.

the convergence of the sequence of objective value $\{g(\mathbf{z}_t)\}_{t\in\mathbb{N}}$, and then convergence of the sequence of variables $\{\mathbf{z}_t\}_{t\in\mathbb{N}}$.

Algorithm 2. Alternate Convex Search Algorithm

1 **Step 1:** Choose a starting point $\mathbf{z}_0 \leftarrow (\mathbf{w}_0, \mathbf{s}_0) \in Z$;
2 Set $t \leftarrow 0$;
3 **while** *not converged* **do**
4 **Step 2:** Solve the convex optimization problem for fixed $\mathbf{w}_t$: $\mathbf{s}_{t+1} \leftarrow \min_{\mathbf{s}}\{g(\mathbf{w}_t, \mathbf{s}), \mathbf{s} \in Z_{\mathbf{w}_t}\}$;
5 **Step 3:** Solve the convex optimization problem for fixed $\mathbf{s}_{t+1}$: $\mathbf{w}_{t+1} \leftarrow \min_{\mathbf{w}}\{g(\mathbf{w}, \mathbf{s}_{t+1}), \mathbf{w} \in Z_{\mathbf{s}_{t+1}}\}$;
6 **Step 4:** Set $\mathbf{z}_{t+1} \leftarrow (\mathbf{w}_{t+1}, \mathbf{s}_{t+1})$;
7 Set $t \leftarrow t + 1$;
8 **end**

Theorem 1. *Let the STM objective function be $g : Z \rightarrow \mathbb{R}$. Then the sequence of objective value $\{g(\mathbf{z}_t)\}_{t\in\mathbb{N}}$ generated by ACS converges monotonically.*

Proof. The sequence $\{g(\mathbf{z}_t)\}_{t\in\mathbb{N}}$ generated by Algorithm 2 decreases monotonically, because $g(\mathbf{w}^*, \mathbf{s}^*) \leq g(\mathbf{w}, \mathbf{s}^*)$, $\forall \mathbf{w} \in Z_{\mathbf{s}^*}$, and $g(\mathbf{w}^*, \mathbf{s}^*) \leq g(\mathbf{w}^*, \mathbf{s}), \forall \mathbf{s} \in Z_{\mathbf{w}^*}$. In addition, Property 2 shows g is bounded from below. According to Theorem 4.5 in [30], the sequence $\{g(\mathbf{z}_t)\}_{t\in\mathbb{N}}$ converges to a limit real value. □

Theorem 1 only tells the convergence of $\{g(\mathbf{z}_t)\}_{t\in\mathbb{N}}$ but not of $\{\mathbf{z}_t\}_{t\in\mathbb{N}}$. See Example 4.3 in [30] where $\{g(\mathbf{z}_t)\}_{t\in\mathbb{N}}$ converge but $\{\mathbf{z}_t\}_{t\in\mathbb{N}}$ diverge. The following states the condition for the convergence of $\{\mathbf{z}_t\}_{t\in\mathbb{N}}$.

Theorem 2. *Let W and S be closed sets, and $z_t = (\mathbf{w}_t, \mathbf{s}_t)_{t\in\mathbb{N}}$ where $\mathbf{w}_t \in W$ and $\mathbf{s}_t \in S$. The sequence of variables $\{\mathbf{z}_t\}_{t\in\mathbb{N}}$ generated by ACS converge to $\mathbf{z}^* \in W \times S$.*

Proof. This can be proved using Theorem 4.7 in [30]. □

6 STM WITH LABELED TARGET DATA (L-STM)

As discussed above, STM requires no labels from the target subject to personalize a generic classifier. Nevertheless, in many problems one might collect partially labeled data from the target domain, or acquire additional guidance with a few manual labels. Such labels can be considered as the only reference to the target subject and aid the determination of the personalized classifier. This section describes an inductive extension of STM, termed *L-STM*, to adapt target labels for personalizing a classifier.

Given the target data and their labels as $\mathcal{D}^L = \{\mathbf{x}_j^L, y_j^L\}_{j=1}^{n_L}$, $y_j^L \in \{+1, -1\}$, $0 \leq n_L \leq n_{\text{te}}$, we formulate L-STM by introducing an additional regularization term $\Omega_L(\mathcal{D}^L)$ to (1):

$$\min_{f,\mathbf{s}} R_f(\mathcal{D}^{\text{tr}}, \mathbf{s}) + \lambda\Omega_{\mathbf{s}}(\mathbf{X}^{\text{tr}}, \mathbf{X}^{\text{te}}) + \lambda_L\Omega_L(\mathcal{D}^L), \qquad (16)$$

where $\lambda_L > 0$ is a tradeoff parameter. A choice of large λ_L ensures the labeled target data are correctly classified. The goal of $\Omega_L(\mathcal{D}^L)$ is to regulate the classification quality on the labeled target data. In this paper, we define $\Omega_L(\mathcal{D}^L) = \sum_{j=1}^{n_L} L^p(y_j^L, f(\mathbf{x}_j^L))$. Note that an L^2 loss here is analogous to the regularization in Least Square SVM [69], which performs comparably with SVM using the hinge loss and has been shown to benefit binary classification, such as our task at hand. Because $\Omega_L(\mathcal{D}^L)$ is convex in f, problem (16) remains a biconvex optimization problem, and thus the ACS algorithm can be directly applied.

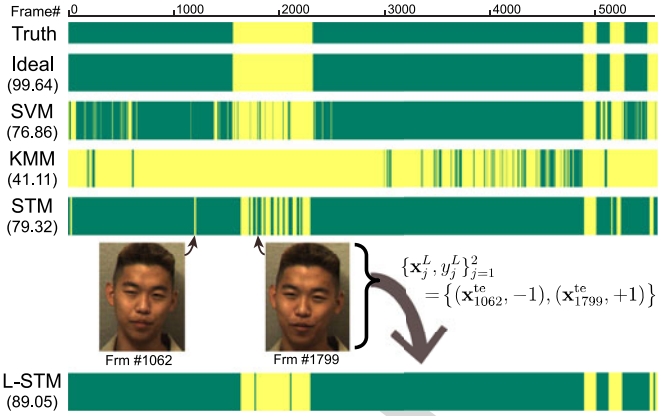

Fig. 6. Comparison of different methods on the RU-FACS dataset. Light yellow (dark green) indicates AU 12 presense (absense) of Subject 12. The numbers in parentheses are F1 scores. Two misclassified frames of STM were chosen and fed into L-STM with correct labels.

We show that solving problem (16) is equivalent to solving the original STM using a training set augmented with weighted labeled target data. We demonstrate the use of L^2 loss on linear SVM, while different choices of loss functions (e.g., L^1) and classifier types (e.g., nonlinear SVM) can be applied. Specifically, updating for $\mathbf{s}$ remains the same process. For updating $\mathbf{w}$, one can use Newton's method by associated gradient and Hessian:

$$\nabla_{\mathbf{w}} = \mathbf{w} + \widehat{\mathbf{X}}\widehat{\mathbf{S}}(\widehat{\mathbf{X}}^\top\mathbf{w} - \widehat{\mathbf{y}}), \qquad (17)$$

$$\mathbf{H}_{\mathbf{w}} = \mathbf{I}_d + \widehat{\mathbf{X}}\widehat{\mathbf{S}}\widehat{\mathbf{X}}^\top, \qquad (18)$$

where $\widehat{\mathbf{X}} = [\mathbf{X}^{\text{tr}}|\mathbf{X}^L]$ is the augmented set with labeled target data, $\widehat{\mathbf{S}} = \begin{bmatrix} 2C\mathbf{S}^0 & 0 \\ 0 & \lambda_L\mathbf{I}_{n_L} \end{bmatrix}$ is the augmented re-weighting matrix, and $\widehat{\mathbf{y}} = \begin{bmatrix} \mathbf{y} \\ \mathbf{y}^L \end{bmatrix}$ are the augmented labels.

The equivalence between (16) and an augmented STM is useful particularly for the scenario of AU detection, where FACS coding is time-consuming and unlabeled videos are usually abundant. L-STM allows users to add just a few frames to alleviate false detections significantly. Fig. 6 illustrates the benefits of L-STM over alternative methods. Light yellow (dark green) indicates positive (negative) frames for AU 12 on Subject 12 of the RU-FACS dataset. Top two rows show the ground truth and the detection result of an ideal classifier. The numbers in parentheses indicate F1 scores. The third and fourth rows illustrate the detection of a generic SVM and KMM. Both approaches produced many false detections due to the person-specific biases and the lack of weight refinement. STM, on the fifth row, greatly reduced false positives and produced a better F1 score. The last row shows the detection of L-STM *only* two misclassified frames from STM with manually corrected labels. L-STM boosted ~10-point F1 score. As we observed empirically, the more the labeled target data are introduced, the better L-STM approaches the ideal classifier.

TABLE 3
Compare STM with Related Transductive Transfer Learning Methods

Methods	Importance re-weight	Weight refine	Convexity	Labeled target data
SVM-KNN [81]	×	×	NA	×
T-SVM [17]	×	×	non-convex	×
KMM [31]	✓	×	convex	×
DA-SVM [6]	×	✓	non-convex	×
DT-MKL [22]	×	×	jointly convex	optional
DAM [23]	×	×	convex	optional
STM (proposed)	✓	✓	bi-convex	optional

✓: *included*, ×: *omitted*, *NA: not applicable*

7 Discussion of Related Work

A few related efforts use *personalized modeling* for facial expression analysis, e.g., AU intensity estimation [53]. STM differs from them in how it accomplishes personalization. Chang and Huang [8] introduced an additional face recognition module and trained a neural network on the combination of face identities and facial features. Romera-Paredes et al. [51] applied multi-task learning to learn a group of linear models and then calibrated the models toward the target subject using target labels. By contrast, STM requires neither a face recognition module nor target labels. Motivated by covariate shift [63], Chen et al. [14] proposed transductive and inductive transfer algorithms for learning person-specific models. In their transductive setting, KL-divergence was used to estimate sample importance. However, STM models the domain mismatch using KMM [31], which with proper tuning, as implied in [64], yields better estimation.

Closest to STM is *transductive transfer learning*, which seeks to address domain shift problems without target labels. Table 3 summarizes the comparison. DT-MKL [22] simultaneously minimizes the MMD criterion [5] and a multi-kernel SVM. DAM [23] leverages a set of pre-trained base classifiers and solves for a test classifier that shares similar predictions with the base classifiers. However, similar to T-SVM [36] and SVM-KNN [81], these methods treat training data uniformly. By contrast, KMM [31] and STM consider importance re-weighting, properly adjusting the importance for each training instance to move the decision function toward test data. KMM performs re-weighting only once while STM does so in an iterative manner. From this perspective, KMM can be viewed as an initialization of STM (see Section 4). In addition, STM uses training loss to refine instance weights in successive steps, thus being able to reduce weights of the samples that carry a large loss. DA-SVM [6] refines instance weights as a quadratic function decaying with iterations. However, DA-SVM could fail to converge due to its non-convexity, while STM is formulated as a bi-convex problem and thus assures convergence. Moreover, STM can be extended to tackle labeled target data, which greatly improves the performance.

8 Experiments

STM was evaluated in datasets that afforded inclusion of both posed and unposed facial expression, frontal versus variable pose, complexity (e.g., interview versus three-person interaction), and differences in numbers of subjects, the amount of video per subject, and men and women of diverse ethnicity. These factors are among the individual differences that adversely affect classifier performance in previous work [28]. We compared STM against alternative approaches under various scenarios, including a generic classifier, person-specific classifiers, and cross-domain classifiers, under within-subject, cross-subject, and cross-dataset scenarios. Operational parameters for STM included initialization order, parameter choice, and domain size.

8.1 Dataset Description

We tested the algorithms on four diverse datasets that involve posed, acted, or spontaneous expressions, and vary in video quality, length, annotation, the number of subjects, and context, as summarized in Table 4 and illustrated in Fig. 7.

(1) The extended Cohn-Kanade (CK+) dataset [44] contains brief (approximately 20 frames on average) videos of posed and un-posed facial expressions. Videos begin with a neutral expression and finish at the apex, or peak, which is annotated with AUs and with holistic expressions. Changes in pose and illumination are relatively small. Posed expressions from 123 subjects and 593 videos were used. Since STM requires some number of frames to estimate a test distribution, it is necessary to modify coding in CK+. Specifically, we assume the last one-third frames share the same AU labels. We note that this may introduce some errors, compared to related methods that use only the peak frame for classification.

(2) The GEMEP-FERA dataset [67] consists of seven portrayed emotion expressions by 10 trained actors. Actors were instructed to utter pseudo-linguistic phoneme sequences or a sustained vowel and display pre-selected facial expressions. Head pose is primarily frontal with some fast movements. Each video is annotated with AUs and holistic expressions. We used the GEMEP-FERA training set, which comprises 7 subjects (three of them men) and 87 videos.

TABLE 4
Detailed Content of Different Datasets

Datasets	#Subjects	#Videos	#Frames/video	Content	AU annotation	Expression annotation
CK+ [44]	123	593	∼20	Neutral→peak	Per video	Per video
GEMEP-FERA [67]	7	87	20∼60	Acting	Frame-by-frame	Per video
RU-FACS [4]	34	34	5000∼8000	Interview	Frame-by-frame	–
GFT [57]	720	720	∼60,000	Multi-person social interaction	Frame-by-frame	–

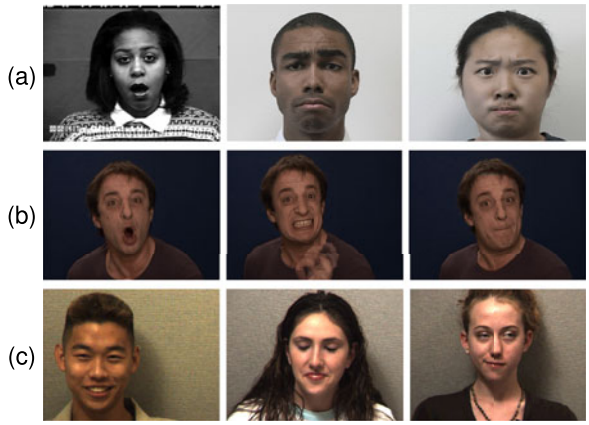

Fig. 7. Example images from (a) CK+ [44], (b) GEMEP-FERA [67], and (c) RU-FACS [4] datasets.

(3) RU-FACS dataset [4] consists of video-recorded interviews of 100 young adults of varying ethnicity. Interviews are approximately 2.5 minutes in duration. Head pose is frontal with small to a moderate out-of-plane rotation. AU are coded if the intensity is greater than 'A', i.e., lowest intensity on a 5-point scale. We had access to 34 of the interviews, of which video from five subjects could not be processed for technical reasons. Thus, the experiments reported here were conducted with data from 29 participants with more than 180,000 frames in total.

(4) GFT [57] consists of social interaction between 720 previously unacquainted young adults that were assembled into groups of three persons each and observed over the course of a 30-minute group formation task. Two minutes of AU-annotated video from 14 groups (i.e., 42 subjects) was used in the experiments for a total of approximately 302,000 frames. Head pose varies over a range of about plus/minus 15-20 degrees [28]. For comparability with RU-FACS, we included AU 6, 9, 12, 14, 15, 20, 23 and 24.

Out of these datasets, CK+ is the most controlled, followed by GEMEP-FERA. Both include annotations for holistic expressions and AUs. GEMEP-FERA introduces variations in spontaneous expressions and large head movements but contains only seven subjects. RU-FACS and GFT are both unposed and vary in complexity. RU-FACS is an interview context; GFT is a social interaction over a longer duration with greater variability. The first sets of experiments focus on CK+, GEMEP, and RU-FACS. GFT figures primarily in experiments on domain transfer between datasets and on the influence of numbers of subjects on performance.

8.2 Settings

Face tracking and registration. For CK+, FERA, and GFT, 49 landmarks were detected and tracked using the Supervised Descent Method (SDM) [74]. For RU-FACS, we used available AAM detection and tracking of 68 landmarks. Tracked landmarks were registered to a 200×200 template shape.

Feature extraction. Given a registered facial image, SIFT descriptors were extracted using 36×36 patches centered at selected landmarks (nine on the upper face and seven on the lower face), because AUs occur only in local facial regions. The dimensionality of the descriptors was reduced by preserving 98 percent PCA energy.

AU selection and evaluation. Positive samples were taken as frames with an AU presence and negative samples as frames without an AU. We selected the eight most commonly observed AUs across all datasets. To provide a comprehensive evaluation, we reported both Area Under the ROC Curve (AUC) and F1 score. As AUC was originally designed for balanced binary classification tasks, F1 score, as the harmonic mean of precision and recall, could be more meaningful for imbalanced data, such as AUs.

Dataset split and validation. A leave-one-subject-out protocol was used. For each AU, we iteratively chose one subject for testing and the remaining subjects for training and validation. For all iterations, we first identified the range for which F1 scores on the validation set was greatest. Then, we chose the F1 scores for which C was small. That is, we sought the parameters that maximize F1 scores while preserving the smoothness of the decision boundary.

8.3 Action Unit (AU) Detection

We evaluated STM with generic classifiers and alternative approaches using three scenarios for AU detection: *within-subject*, *cross-subject*, and *cross-dataset*. We report results separately for each scenario.

8.3.1 Within-Subject AU Detection

A natural comparison with STM is a classifier trained on a single subject, also known as a *Person-Specific (PS)* classifier. A PS classifier can be defined in at least two ways. One, the more common definition, is a classifier trained and tested on the same subject. We refer to this usage as PS_1. The other definition, referred to as PS_2 or *quasi-PS*, is a classifier that has been tested on a subject included in the training set. The GEMEP-FERA competition [67] defined PS in this way. An SVM trained with PS_2 (PS_2-SVM) is sometimes considered to be a generic classifier (e.g., [45]). In our usage, we reserve the term "generic classifier" to the case in which training and test subjects are independent.

Here we compare STM with both PS_1-SVM and PS_2-SVM, and summarize the results in Table 5. In all, PS_1-SVM showed the lowest AUC and F1. This outcome occurred because of the relatively small number of samples for individual subjects. Lack of sufficient training data for individual subjects is a common problem for person-specific classifiers. It is likely that PS_1-SVM would have performed the best if the amount training data from the same subject is large enough. PS_2-SVM achieved better AUC and F1 because it sees more training subjects. Overall, STM consistently outperformed both PS classifiers.

Selection ability of STM. Recall that PS_2 includes samples of the test subject in both training and test sets. Could STM improve PS_2 performance by selecting proper training samples? To answer this question, we employed PS_2 to investigate STM's ability to select *relevant* training samples with respect to the test subject. Table 6 shows the selection percentage of STM upon initialization and convergence. Here STM is initialized by KMM. Each row sums to 1 and represents a test subject; each entry within one row denotes the percentage of selected samples from each training subject. For example, (a) shows the initialization phase that, when testing on Subject 2, 26 percent of training samples

TABLE 5
Within-Subject AU Detection with STM and PS Classifiers

	AUC			F1 Score		
AU	PS_1-SVM	PS_2-SVM	STM	PS_1-SVM	PS_2-SVM	STM
1	48.0	72.4	**79.2**	45.0	54.8	**61.9**
2	46.5	71.1	**80.2**	45.9	55.7	**64.3**
4	62.6	61.9	**66.5**	46.6	40.7	**60.4**
6	70.3	80.0	**86.4**	60.2	69.7	**78.5**
7	47.5	54.3	**72.4**	49.4	55.3	**58.4**
12	65.7	74.0	**72.3**	69.5	70.4	**72.6**
15	41.4	64.0	**70.5**	44.5	49.0	**56.0**
17	32.6	**70.3**	61.7	25.0	**40.3**	36.3
Av.	51.8	68.5	**73.6**	48.3	54.5	**61.0**

TABLE 6
Selection Percentage of STM for Different Subjects

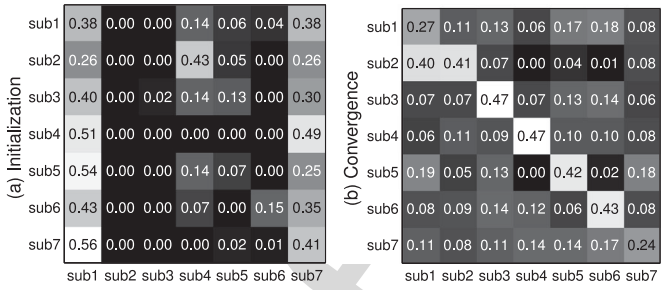

were selected from Subject 1. Upon convergence, as (b) shows, STM selected most training samples that belong to the target subject (higher diagonal value). Note that the selection percentages along the diagonal do not sum to 100 percent due to insufficient training samples for the target subject. As a result, STM was able to select relevant training samples, even from different subjects, to alleviate the mismatch between training and test distributions.

8.3.2 Cross-Subject AU Detection

Using a cross-subject scenario, i.e., training and test subjects are independent in all iterations (a.k.a., *leave-one-subject-out*), we compared STM against various types of methods. Unsupervised domain adaptation methods are closest to STM. For comparisons we included Kernel Mean Matching (KMM) [31], Domain Adaptation SVM (DA-SVM) [6], and Subspace Alignment (SA) [25]. Multiple source domain adaptation methods serve as another natural comparison by treating each training subject as one source domains; we compared to the state-of-the-art DAM [23]. For baseline methods, we compared with linear SVMs and semi-supervised Transductive SVM (T-SVM) [17]. T-SVM, KMM, DAM and SA were implemented per the respective author's webpage. Because STM requires no target labels, methods that use target labels for adaptation (e.g., [19], [40], [54]) were not included.

All methods were compared in CK+ and RU-FACS with a few exceptions in CK+. In CK+, SA was ruled out because too few frames were available per subject to compute meaningful subspaces. DAM was also omitted in CK+ because it would be problematic to choose negative samples given the structure of the data (i.e., pre-segmented positive examples). In training, a Gaussian kernel was used with a bandwidth set as the median distance between pairwise samples. For KMM and STM we set $B=1{,}000$ so that none of s_i reached the upper bound, and $\epsilon=\frac{\sqrt{n_{\text{tr}}-1}}{\sqrt{n_{\text{tr}}}}$. As reported in [31], when B was reduced to the point where a small percentage of the $\mathbf{s}_i$ reached B, empirically performance either remained unchanged, or worsened. For T-SVM we used [17] since the original T-SVM [36] solves an integer programming and thus unscalable to our problem that consists hundreds to thousands of frames. For fairness, we used linear SVMs in all cases. In DA-SVM, we used LibSVM [7] as discussed in Section 4, $\tau=0.5$ and $\beta=0.03$. For SA, we obtained the dimension of subspaces d_{max} using their theoretical bound with $\gamma=10^6$ and $\delta=0.1$; SA with both NN and SVM classifiers were reported. Following [23], we tuned DAM using $C=1$, $\lambda_L=\lambda_{D_1}=\lambda_{D_2}=1$; β was set as the median of computed MMD values [5]; the threshold for virtual labels were cross-validated in $\{0.01, 0.1, 0.5, 1\}$. Linear SVMs were used as base classifiers. Note that, because these alternative methods are not optimized for our task, their performances might be improved by searching over a wider range of parameters.

Discussion. Tables 7 and 8 show results on AUC and F1 scores. A linear SVM served as a generic classifier. For semi-supervised learning, T-SVM performed similarly to SVM in RU-FACS, but worse than SVM in CK+. An explanation is that in CK+ the negative (neutral) and positive (peak frames) samples are easier to separate than consecutive frames in RU-FACS. For transductive transfer learning, KMM performed worse than the generic classifier,

TABLE 7
Cross-Subject AU Detection on RU-FACS Dataset. "SA (NN|SVM)" Indicates SA with NN and SVM, Respectively

	AUC							F1 Score						
AU	SVM	KMM	T-SVM	DA-SVM	SA (NN|SVM)	DAM	STM	SVM	KMM	T-SVM	DA-SVM	SA (NN|SVM)	DAM	STM
1	72.0	74.0	72.0	77.0	41.2|82.0	82.6	**83.9**	40.8	37.7	37.4	35.5	20.9|24.2	11.3	**55.3**
2	66.6	58.6	71.1	76.5	38.2|81.4	81.2	**82.4**	35.7	32.2	36.2	34.1	18.6|21.8	17.0	**52.6**
4	74.8	62.2	50.0	76.4	24.5|71.1	51.3	**82.4**	25.2	14.5	11.2	**35.3**	5.7| 5.8	2.9	30.4
6	89.1	88.8	61.6	60.3	46.2|78.3	81.2	**93.1**	58.3	39.2	33.1	42.9	23.2|19.2	20.9	**72.4**
12	86.7	87.0	86.7	84.4	55.9|86.1	**93.1**	92.3	61.9	63.0	62.6	71.4	37.5|38.6	36.6	**72.3**
14	71.8	67.8	74.4	70.4	38.0|78.5	79.5	**87.4**	31.3	25.8	25.8	40.9	16.5|15.7	5.7	**51.0**
15	72.5	68.8	73.5	58.1	37.7|79.2	71.8	**86.1**	32.3	29.5	32.3	34.9	10.1| 8.8	3.2	**45.4**
17	78.5	76.7	79.5	75.7	55.8|89.9	**93.9**	89.6	39.5	35.6	44.0	46.5	21.9|17.2	22.9	**55.3**
Av.	76.5	72.3	71.1	72.3	42.2|80.8	79.3	**86.3**	40.6	37.3	40.6	42.7	19.3|18.9	15.1	**54.3**

TABLE 8
Cross-Subject AU Detection on CK+ Dataset

	AUC					F1 Score				
AU	SVM	KMM	T-SVM	DA-SVM	STM	SVM	KMM	T-SVM	DA-SVM	STM
1	79.8	68.9	69.9	72.6	**88.9**	61.1	44.9	56.8	57.7	**62.2**
2	**90.8**	73.5	69.3	71.0	87.5	73.5	50.8	59.8	64.3	**76.2**
4	74.8	62.2	63.4	69.9	**81.1**	62.7	52.3	51.9	57.7	**69.1**
6	89.7	87.7	60.5	**94.7**	94.0	75.5	70.1	47.8	68.2	**79.6**
7	82.1	68.2	55.7	61.4	**91.6**	59.6	47.0	43.8	53.1	**79.1**
12	88.1	89.5	76.0	**95.5**	92.8	76.7	74.5	59.6	59.0	**77.2**
15	93.5	66.8	49.9	94.1	**98.2**	75.3	44.4	40.4	76.9	**84.8**
17	90.3	66.6	73.1	94.7	**96.0**	76.0	53.2	61.7	81.4	**84.3**
Av.	86.1	72.9	64.7	81.7	**91.3**	70.0	54.7	52.7	64.8	**76.6**

because KMM estimates sample weights without label information. SA combined with both Nearest Neighbor (NN) and SVM led to even worse results than the above methods. This is because SA obtains an optimal transformation through linear subspace representation, which could be improper due to the non-linearity of our data. In addition, SA weighted all training samples equally, and thus suffered from biases caused by individual differences (as illustrated in Fig. 2). Although SA+SVM performed better in AUC, its low F1 score tells a likely overfitting (low precision or recall). The proposed STM outperformed alternative methods in general. For AUC in RU-FACS, STM achieved the highest averaged score about 6 points higher than the 2nd best, and the highest scores in all but two AUs. For F1, STM had the highest averaged score about 12 points higher than the nearest alternative, and the highest F1 score of all but AU4. For CK+, STM achieved 91 percent AUC on average, slightly better than the best-published result 90.5 percent [41], although the results may not be directly comparable due to different choices of features and registration. It is noteworthy that we tested the last one-third of a video that could contain low intensities, while [41] tested only on peak frames with the highest intensity. On the other hand, STM may be benefited from additional frames due to more information.

For other SVM-based methods, unlike STM that uses a penalized SVM, T-SVM considered neither re-weighting for training instances nor weight refinement for irrelevant samples, such as noises or outliers. On the other hand, DA-SVM extends T-SVM by progressively labeling test samples and removing labeled training ones. Not surprisingly, DA-SVM showed better performance than KMM and T-SVM, because it selects relevant samples for training. However, similar to T-SVM, DA-SVM did not update the re-weightings using label information. Moreover, it is not always guaranteed to converge. In our experiments, we faced the situation where DA-SVM failed to converge due to a large amount of samples lying within the margin bounds. In contrast, STM is a biconvex formulation, and therefore is guaranteed to converge to a critical point and outperformed existing approaches (details in Section 4).

As for multi-source domain adaptation, DAM overall performed comparably in AUC, but significantly worse than STM in F1. There are at least three explanations. First, AUs are by nature imbalanced: Simply predicting all samples as negative could yield high AUC for infrequent AUs (such as AUs 4), yet zero precision and recall for F1 score. Second, similar to person-specific classifiers, training samples for each subject are typically insufficient to estimate the true distribution (as discussed in Section 8.3.1). Using such limited training samples for each subject, therefore, limits the power of base classifiers and the final prediction in DAM. Last but not least, DAM uses MMD to estimate inter-subject distance, which could be inaccurate due to insufficient samples or sampling bias (e.g., some subjects have more expressions than others).

Although in Table 7 STM achieved slightly worse than DAM in AUC for some AUs, STM showed a better improvement in F1 metric, which more properly describes our imbalanced detection task. STM's improvement could be limited due to insufficient training subjects, which hinder STM from selecting and receiving proper supports from the training samples. This can be also explained by the findings of selection ability in Section 8.3.1. When the number of subjects and training samples increase, as will be illustrated in Section 8.5.3, STM is able to gain contributions from the selected data, and thus the improvement becomes more obvious. Overall STM achieved the most competitive performance due to the properties of instance re-weighting, weight refinement, and convergence.

8.3.3 Cross-Dataset AU Detection

Detecting AUs across datasets is challenging because of differences in acquisition and participant characteristics and behavior. Fig. 7 shows participant characteristics, context, illumination, camera parameters among the differences that may bias features. Generic SVMs fail to address such differences. Sections 8.3.1 and 8.3.2 have shown the effectiveness of STM on *within-dataset* experiments involving within-subject and across-subject scenarios. This section aims to justify that STM can attain not only subject adaptation but can be naturally extended for *cross-dataset* adaptation. Specifically, we performed two experiments, RU-FACS→GEMEP-FERA and GFT→RU-FACS, using the same settings described above.

Table 9 shows the results. One can observe that cross-domain approaches outperformed a generic classifier in most cases. It is not surprising because a generic classifier does not model the biases between datasets. That is, in the cross-dataset scenario, the training and test distributions vary more dramatically than in within-dataset scenario, causing a generic classifier to fail to transfer the knowledge from one dataset to another. This also explains why cross-domain approaches showed consistent improvements in the cross-dataset setting, compared to the within-dataset results. Among the cross-domain methods, STM consistently outperforms the others. Observe STM gained improvement over SVM in Table 7 by 12.8 percent in AUC (76.5→86.3) and 33.7 percent in F1 (40.6→54.3), and in Table 9(b) by 37.9 percent in AUC (55.8→77.0) and 46.1 percent in F1 (28.6→41.8). The advantages of STM over SVM becomes more obvious in the cross-dataset experiments.

8.4 Holistic Expression Detection

Taking into account of individual differences, STM showed improvement for AU detection. In this experiment, we ask whether the same could be found for holistic expression

TABLE 9
Cross-Dataset AU Detection: (a) RU-FACS→GEMEP-FERA, and (b) GFT→RU-FACS
("A→B" Represents for Training on Dataset A and Test on B)

(a)	AUC					F1 Score				
AU	SVM	KMM	T-SVM	DA-SVM	STM	SVM	KMM	T-SVM	DA-SVM	STM
1	44.7	48.8	43.7	56.9	**63.2**	46.3	46.4	41.8	46.1	**50.4**
2	52.8	70.5	52.1	52.3	**74.0**	47.4	54.2	38.6	45.4	**54.6**
4	52.7	55.4	54.2	52.7	**58.6**	57.1	57.1	40.2	42.9	**57.4**
6	73.5	55.2	77.1	79.9	**83.4**	60.7	55.2	52.8	56.3	**72.7**
12	56.8	60.1	70.9	76.1	**78.1**	67.7	67.7	63.5	62.6	**71.5**
15	55.1	52.1	59.3	**60.2**	58.6	31.5	32.8	29.7	26.4	**41.1**
17	44.3	41.1	39.1	46.2	**52.7**	27.3	27.1	24.3	24.6	**31.4**
Av.	54.3	54.8	56.6	60.6	**66.9**	48.3	48.6	41.6	43.5	**54.2**

(b)	AUC					F1 Score				
AU	SVM	KMM	T-SVM	DA-SVM	STM	SVM	KMM	T-SVM	DA-SVM	STM
1	45.8	63.6	70.3	71.2	**73.7**	23.7	29.8	26.6	31.8	**38.6**
2	46.4	62.8	68.5	68.2	**71.7**	21.3	25.4	19.4	**32.1**	30.2
4	56.9	60.1	59.1	47.2	**61.7**	18.3	24.5	20.7	19.4	**28.5**
6	65.5	73.9	81.5	74.1	**93.3**	42.2	46.8	30.4	38.7	**61.4**
12	65.3	72.1	76.3	80.9	**90.3**	43.2	47.6	45.8	56.8	**62.2**
14	57.2	54.8	53.7	70.2	**72.2**	25.8	23.8	25.9	29.7	**36.2**
15	56.9	61.8	64.2	65.5	**80.4**	23.7	30.3	28.2	29.9	**37.8**
17	52.4	54.5	64.8	**72.6**	**72.6**	30.8	31.5	32.3	38.9	**39.5**
Av.	55.8	62.9	67.3	68.7	**77.0**	28.6	32.5	28.7	34.7	**41.8**

detection. We used the major benchmarks CK+ [44] and FERA emotion subchallenge [67] for this experiment, and the same settings in Section 8.2, except for that the labels were replaced as holistic expressions. Similar to [67], we utilized every frame of a video to train and test our algorithm. Because each video had only a single expression label instead of a frame-by-frame labeling, F1 score is meaningless in this experiment. For CK+, 327 out of the original 593 videos were given a nominal expression label based on the 7 basic and discrete expressions: *Anger*, *Contempt*, *Disgust*, *Fear*, *Happy*, *Sadness*, and *Surprise*. For GEMEP-FERA, 289 portrayals were retained one out of the five expression states: *Anger*, *Fear*, *Joy*, *Sadness*, and *Relief*. The training set included seven actors with 3∼5 instances of each expression per actor. We evaluated on the training set, which contained a total of 155 videos. STM was also compared to alternative approaches discussed in Section 8.3.2.

Table 10(a) shows the results from CK+. Note that DA-SVM is unavailable in this experiment because it failed to converge to a final classifier due to insufficient test data, recalling that we used the last one-third frames of each video for test. One can observe that a generic SVM performed fairly well because positive (peak expressions) and negative samples (neutral faces) are relatively easy to separate in CK+. KMM and T-SVM resulted in suboptimal results due to the lack of a weight-refinement step, and thus were unable to rectify badly estimated weights for learning the final classifier (see discussions in Section 7). This effect becomes obvious when there is insufficient test data, such as this experiment. On the other hand, STM considers the labels for weight refinement and performed similarly as well as a generic SVM.

Table 10(b) presents our results on GEMEP-FERA, which served as a larger and more challenging benchmark for evaluating the holistic expression detection performance. In this experiment, each test video consisted of tens of frames, and thus enabled DA-SVM to converge in most cases. The generic SVM performed poorly due to large variations in this dataset, such as head movements and exaggerated expressions. Without the ability to select meaningful training samples, the generic classifier suffered from the individual differences. Other cross-domain methods alleviated the person-specific biases and produced better results. Overall STM achieved the best averaged performance. This also serves as evidence that when training data grow larger and more complex, the improvement of STM becomes clearer.

8.5 Analysis

8.5.1 Initialization Order

A potential concern of STM is that the initialization order could affect the convergence property and performance. To evaluate this, we examined the initialization order with $\mathbf{w}_0$ ($\text{STM}_\mathbf{w}$) and with $\mathbf{s}_0$ ($\text{STM}_\mathbf{s}$). Standard two-stage approach, i.e., solving the selection coefficients first and then the penalized SVM (e.g., [31]), can be interpreted as $\text{STM}_\mathbf{w}$, as discussed in Section 4. To validate convergence property of STM, we randomized 10 initialization sets for $\text{STM}_\mathbf{w}$ and $\text{STM}_\mathbf{s}$ respectively. Upon the convergence of STM, we computed the objective differences in consecutive iterations ($g(\mathbf{z}_{t+1}) - g(\mathbf{z}_t)$), and the absolute sum of variable difference ($\|\mathbf{z}_{t+1} - \mathbf{z}_t\|_1$). For the cases where STM took fewer iterations to converge, we set the difference of later iterations to 0.

Fig. 8a shows the curve of mean and standard deviation of differences across the iterations of $\text{STM}_\mathbf{w}$ and $\text{STM}_\mathbf{s}$. Note that the differences were scaled for visualization convenience. The random initial value was reflected in the first iteration and made a major difference with the value of the second iteration. One can

TABLE 10
Expression Detection with AUC on (a) CK+ and (b) GEMEP-FERA

(a) CK+

Expression	SVM	KMM	T-SVM	DA-SVM	STM
Anger	95.1	85.3	76.1	–	**96.4**
Contempt	**96.9**	94.5	88.8	–	**96.9**
Disgust	94.5	81.6	84.2	–	**96.0**
Fear	**96.6**	92.7	84.9	–	95.5
Happy	**99.4**	93.9	86.7	–	98.9
Sadness	**94.5**	76.0	78.7	–	93.3
Surprise	97.3	64.5	81.8	–	**97.6**
Av.	96.3	84.1	83.0	–	**96.4**

(b) GEMEP-FERA

Expression	SVM	KMM	T-SVM	DA-SVM	STM
Anger	31.1	66.5	70.4	**78.8**	78.6
Fear	31.9	81.4	64.5	83.9	**85.5**
Joy	90.2	33.5	78.9	71.1	**95.0**
Relief	20.4	74.8	76.8	87.9	**88.4**
Sadness	73.4	80.2	77.1	74.7	**84.8**
Av.	49.4	67.3	73.5	79.3	**86.5**

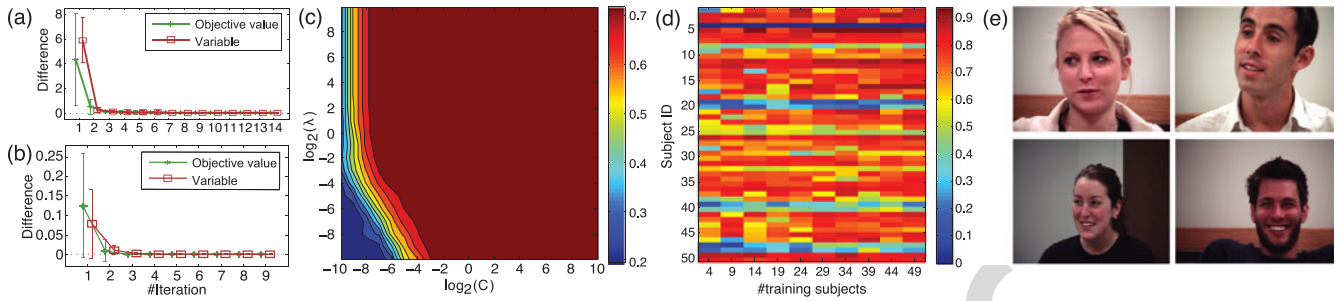

Fig. 8. Analysis experiments: (a)–(b) Objective and variable differences between iterations with initialization $\mathbf{w}_0$ ($\text{STM}_\mathbf{w}$) and $\mathbf{s}_0$ ($\text{STM}_\mathbf{s}$), respectively. (c) Performance versus parameter choices. (d) Per-subject F1 score versus # training subjects. (e) Exemplar images of the GFT dataset [57].

observe that in $\text{STM}_\mathbf{w}$ and $\text{STM}_\mathbf{s}$, both the objective value and difference between consecutive variables decreased at each step and toward convergence, as theoretically detailed in Section 5. Note that, although the resulting solution was slightly different due to different initialization, the performance remains the same as both converge to a critical point. We observed so by comparing the confusion matrices during the experiments.

8.5.2 Parameter Choice

Recall that training STM involves two parameters: C for the tradeoff between maximal margin and training loss, and λ for the tradeoff between the SVM empirical risk and the domain mismatch. This section examines the sensitivity of performance with respect to different parameter choices. Specifically, we ran the experiments of detecting AU12 on the CK+ dataset with the parameters ranges $C \in \{2^{-10}, \ldots, 2^{10}\}$ and $\lambda \in \{2^{-10}, \ldots, 2^{10}\}$. Following the experiment settings in Section 8.2, we computed an averaged F1 score for evaluating the performance. We used Gaussian kernel with a fixed bandwidth as the median distance between sample points.

Fig. 8c illustrates the contour plot of F1 score versus different parameter pairs in terms of $(\log_2(C), \log_2(\lambda))$. As can be observed, the performance scatters evenly in most region of the plot, showing that STM is robust to the parameter choices when their values are reasonable. The performance decayed when both (C, λ) become extremely small ($< 2^{-6}$), as shown in the bottom left of the plot. This is not surprising because smaller values of C and λ imply less emphasis on training loss and personalization. Note that with large enough λ, STM does not need large C to achieve comparable F1, providing an explanation that personalization helps avoid imposing large C and hence avoids overfitting. As a general guideline for choosing parameters, we suggest a small value of C with a reasonably large λ (thus encouraging a decision boundary with reasonably small distribution mismatch).

We note that cross validation (CV) for domain adaptation methods is difficult and remains an open research issue. As also mentioned in [64], this issue becomes vital in a conventional scenario where the number of training samples is much smaller than the number of test samples. However, in our case, we always have much more training samples than test samples, and thus, the CV process is less biased under covariate shift. In addition, as can be seen in Fig. 2 of [64], with proper σ (kernel bandwidth) and standard CV, KMM consistently reaches lower error than the KL-divergence-based CV [64]. This serves as a justification for KMM's ability to estimate importance weights.

8.5.3 Domain Size

The intuition for STM to work better in facial expression analysis is a judicious selection of training samples. Richer diversity grants STM a broader knowledge to select better candidates that match the test distribution. This experiment examines performance changes w.r.t. diversities of the source domain, which we describe as the domain size or the number of training subjects. Intuitively, the larger number of training subjects is, the more diverse the training domain is, and thus the more likely STM could perform better. We compared STM to a generic SVM (with cross-validation) to contrast the performance.

This experiment was performed on AU12 using the RU-FACS dataset. A subset from 3 to 27 training subjects was randomly picked as a shrunk domain. The leave-one-subject-out protocol and F1 score were used following Section 8.2. Fig. 9a illustrates the effects of #training subjects on averaged F1 scores. For each domain size, the mean and standard deviation were computed on F1 scores over all test subjects. Test subjects without true positives were ignored because their precision and F1 scores were not computable.

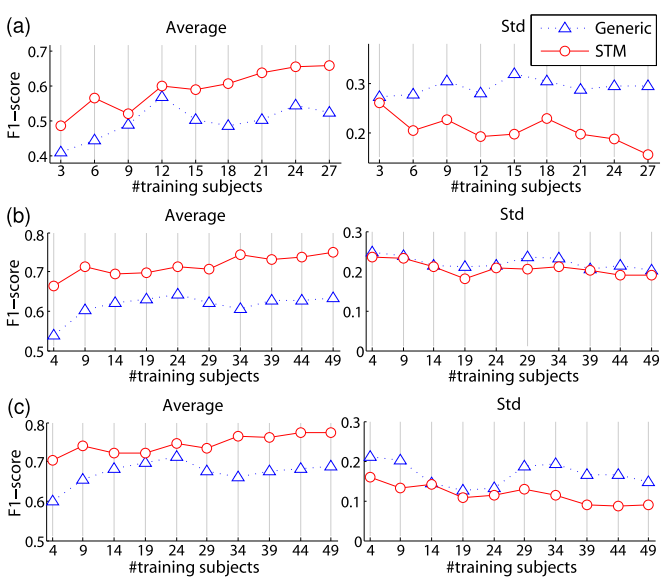

Fig. 9. Performance versus domain size: The averaged and standard deviation of F1 score on (a) RU-FACS. (b) and (c) show the F1 scores on the GFT dataset before and after removing the *outlier* subjects.

One can observe that, as #training subjects grew, STM achieved higher F1 scores, and also performed more consistently with lower standard deviation. This observation imitates Section 8.3.2, where a source domain with poor diversity was shown to limit STM's performance. On the other hand, the generic classifier improved when #training subjects rose to 12. However, with more training subjects being introduced, its performance was slightly lowered due to the biases caused by individual differences. Note that, because the training subjects were downsampled in a randomized manner, it is possible that STM achieved better performance on a domain with less training subjects.

As another justification, we examined the effects of domain size on the GFT dataset [57], which contains a larger number of subjects and more intensive facial expressions than RU-FACS. The GFT dataset records videos of real-life social interactions among three-person groups in less constrained contexts. Videos were recorded using separate wall-mounted cameras facing each subject; Fig. 8e shows exemplar frames. The videos include moderate-to-large head rotations and frequent occlusions; facial movements are spontaneous and unscripted. We selected 50 videos with around 3 minutes each (5,400 frames).

Following the same procedure, we randomly picked a subset of subjects varying from 4 to 49 as the shrunk domains. Fig. 9b shows the F1 scores with respect to the number of training subjects. One can observe the averaged F1 score increased with #training subjects, although the standard deviation fluctuated. To study the fluctuation, we broke down the averaged F1 into individual subjects corresponding to different training sizes, as shown in Fig. 8d. Each row represents a test video; each column represents one number of training subjects (ranging from 4 to 49). Note that for subject four (the 4th row), there is no F1 score because AU12 was absent. One can observe that for six *outlier* subjects (e.g., rows 19, 20, 39, 40, 47, 48), their F1 scores remained low even as the number of subjects was increased. This result suggests that these subjects share no or few instances in the feature space. Visual inspection of their data was consistent with this hypothesis. The outliers were ones with darker skin color, asymmetric smiles or relatively large head pose variations. Thus, for these subjects STM could offer no benefit. This finding suggests the need to include great heterogeneity in training subjects. When these subjects were omitted, as shown in Fig. 9c, the F1 scores are markedly higher. The influence of the domain size becomes clear and replicates Fig. 9a. It is interesting to note that, for generic classifiers, the performance increased until 24 training subjects and then drops abruptly. This observation serves as another evidence that individual differences (introduced by increasing number of training subjects) could bias generic classifiers.

Between these two experiments, generally the averaged F1 score in GFT is higher than that in RU-FACS. At least two factors may have accounted for this difference. One is that participants in GFT may have been less inhibited and more expressive. In RU-FACS, subjects were motivated to convince an examiner of their veridicality. They knew that they would be penalized if they were not believed. In the three-person social interaction of GFT, there were no such negative contingencies. Subjects may have felt more relaxed and become more expressive. More intense AUs are more easily detected. The other factor is that inter-observer reliability of the ground truth FACS labels was likely much higher for GFT than for RU-FACS. Kappa coefficients for GFT were exceptionally good. While reliability for RU-FACS is not available, we know from past confirmation-coding that inter-observer agreement was not as high. Less error in the GFT ground truth would contribute to more accurate classifier performance.

8.6 Discussion

In above experiments, we have evaluated STM against alternative methods in many scenarios: Within-subject (Section 8.3.1), cross-subject (Section 8.3.2), cross-dataset (Section 8.3.3), and holistic expression detection (Section 8.4). We also systematically analyzed STM on its initialization order, and the sensitivity to parameters and domain size (Section 8.5). STM consistently outperformed a generic SVM and most alternative methods. The advantage of STM is clearest in GFT, where the variety of subjects are more extensive, and slightly so, in RU-FACS. The results indicate a more obvious improvement in F1 than in AUC, in large complex datasets than in posed datasets, in cross-dataset scenario than in within-dataset scenario, and with more training subjects than with fewer ones.

STM has some limitations. For example, it suffers from the lack of training subjects or crucial mismatch between training and test distributions, which are known as common drawbacks in unsupervised domain adaptation methods. For a theoretical analysis in terms of performance versus the number of samples, Corollary 1.9 in KMM [29] reaches a transductive bound for an estimated risk of a re-weighted task, given the assumptions of linear loss and data being iid. However, it remains unclear how to theoretically analyze STM's performance in terms of the number of test samples, because STM involves nonlinear loss functions and the data are from real-world videos (non-iid).

9 Conclusion and Future Work

Based on the observation of individuals differences, we have presented Selective Transfer Machine for personalized facial expression analysis. We showed that STM translates to a biconvex problem, and proposed an alternating algorithm with a primal solution. In addition, we introduced L-STM, an extension of STM that exhibited significant improvement when labeled test data are available. Our results on both AU and holistic expression detection suggested that STM is capable of improving test performance by selecting training samples that form a close distribution to test samples. Experiments using within-subject, cross-subject, and cross-dataset scenarios revealed two insights: (1) Some training data are more instrumental than others, and (2) the effectiveness of STM scales as the number of training subjects increases.

It is worth noticing that STM can be extended to other classifiers with convex decision functions and losses, such as logistic regression. This is a direct outcome of Property 1 in Section 5.1. However, for non-convex cases, such as random

forest, local minimum could cause worse performance. We leave extensions to non-convex classifiers as a focus of future work. Moreover, improving STM's training speed could be another direction due to the QP for solving $\mathbf{s}$. Finally, while this study focuses evaluations on facial expressions, STM could be applied to other fields where object-specific issues are involved, e.g., object or activity recognition.

Acknowledgments

The authors would like thank many anonymous reviewers for constructive feedback. Research reported in this paper was supported in part by the National Institutes of Health (NIH) under Award Number R01MH096951, the National Science Foundation (NSF) under the grant RI-1116583, and Army Research Laboratory Collaborative Technology Alliance Program under cooperative agreement W911NF-10-2-0016. The content is solely the responsibility of the authors and does not necessarily represent the official views of the NIH or the NSF.

References

[1] R. Aumann and S. Hart, "Bi-convexity and bi-martingales," *Israel J. Math.*, vol. 54, no. 2, pp. 159–180, 1986.
[2] Y. Aytar and A. Zisserman, "Tabula RASA: Model transfer for object category detection," in *Proc. IEEE Int. Conf. Comput. Vision*, 2011, pp. 2252–2259.
[3] M. Baktashmotlagh, M. T. Harandi, B. C. Lovell, and M. Salzmann, "Unsupervised domain adaptation by domain invariant projection," in *Proc. IEEE Int. Conf. Comput. Vision*, 2013, pp. 769–776.
[4] M. Bartlett, G. Littlewort, M. Frank, C. Lainscsek, I. Fasel, and J. Movellan, "Automatic recognition of facial actions in spontaneous expressions," *J. Multimedia*, vol. 1, no. 6, pp. 22–35, 2006.
[5] K. M. Borgwardt, A. Gretton, M. J. Rasch, H. P. Kriegel, B. Schölkopf, and A. J. Smola, "Integrating structured biological data by kernel maximum mean discrepancy," *Bioinformatics*, vol. 22, no. 14, pp. 49–57, 2006.
[6] L. Bruzzone and M. Marconcini, "Domain adaptation problems: A DASVM classification technique and a circular validation strategy," *IEEE Trans. Pattern Anal. Mach. Intell.*, vol. 32, no. 5, pp. 770–787, May 2010.
[7] C.-C. Chang and C.-J. Lin, "LIBSVM: A library for support vector machines," *ACM Trans. Intell. Syst. Technol.*, vol. 2, pp. 27:1–27:27, 2011.
[8] C.-Y. Chang and V.-C. Huang, "Personalized facial expression recognition in indoor environments," in *Proc. Int. Joint Conf. Neural Netw.*, 2010, pp. 1–8.
[9] K.-Y. Chang, T.-L. Liu, and S.-H. Lai, "Learning partially-observed hidden conditional random fields for facial expression recognition," in *Proc. IEEE Conf. Comput. Vis. Pattern Recog.*, 2009, pp. 533–540.
[10] Y. Chang, C. Hu, R. Feris, and M. Turk, "Manifold based analysis of facial expression," *Image Vision Comput.*, vol. 24, no. 6, pp. 605–614, 2006.
[11] O. Chapelle, "Training a support vector machine in the primal," *Neural Comput.*, vol. 19, no. 5, pp. 1155–1178, 2007.
[12] R. Chattopadhyay, Q. Sun, W. Fan, I. Davidson, S. Panchanathan, and J. Ye, "Multi-Source domain adaptation and its application to early detection of fatigue," *ACM Trans. Knowl. Discovery Data*, vol. 6, no. 4, p. 18, 2012.
[13] J. Chen, M. Kim, Y. Wang, and Q. Ji, "Switching Gaussian process dynamic models for simultaneous composite motion tracking and recognition," in *Proc. IEEE Conf. Comput. Vis. Pattern Recog.*, 2009, pp. 2655–2662.
[14] J. Chen, X. Liu, P. Tu, and A. Aragones, "Learning person-specific models for facial expression and action unit recognition," *Pattern Recog. Lett.*, vol. 34, no. 15, pp. 1964–1970, 2013.
[15] S. W. Chew, P. Lucey, S. Lucey, J. Saragih, J. F. Cohn, and S. Sridharan, "Person-independent facial expression detection using constrained local models," in *Proc. IEEE Int. Conf. Autom. Face Gesture Recog.*, 2011, pp. 915–920.
[16] S. W. Chew, P. Lucey, S. Lucey, J. Saragih, J. F. Cohn, I. Matthews, and S. Sridharan, "In the pursuit of effective affective computing: The relationship between features and registration," *IEEE Trans. Syst., Man, Cybern., Part B: Cybern.*, vol. 42, no. 4, pp. 1006–1016, Aug. 2012.
[17] R. Collobert, F. Sinz, J. Weston, and L. Bottou, "Large scale transductive SVMs," *J. Mach. Learning Res.*, vol. 7, pp. 1687–1712, 2006.
[18] T. F. Cootes, G. J. Edwards, and C. J. Taylor, "Active appearance models," *IEEE Trans. Pattern Anal. Mach. Intell.*, vol. 23, no. 6, pp. 681–685, Jun. 2001.
[19] H. Daumé III, "Frustratingly easy domain adaptation," in *Proc. Conf. Assoc. Comput. Linguistics*, 2007, pp. 256–263.
[20] F. De la Torre and J. F. Cohn, "Facial expression analysis," *Visual Analysis of Humans: Looking at People*, p. 377, 2011.
[21] X. Ding, W.-S. Chu, F. De la Torre, and J. F. Cohn, "Facial action unit event detection by cascade of tasks," in *Proc. IEEE Int. Conf. Comput. Vis.*, 2013, pp. 2400–2407.
[22] L. Duan, I. W. Tsang, and D. Xu, "Domain transfer multiple kernel learning," *IEEE Trans. Pattern Anal. Mach. Intell.*, vol. 34, no. 3, pp. 465–479, Mar. 2012.
[23] L. Duan, D. Xu, and I. W. Tsang, "Domain adaptation from multiple sources: A domain-dependent regularization approach," *IEEE Trans. Neural Netw. Learning Syst.*, vol. 23, no. 3, pp. 504–518, Mar. 2012.
[24] M. Dudık, R. E. Schapire, and S. J. Phillips, "Correcting sample selection bias in maximum entropy density estimation," in *Proc. Adv. Neural Inf. Process. Syst.*, 2005, pp. 323–330.
[25] B. Fernando, A. Habrard, M. Sebban, and T. Tuytelaars, "Unsupervised visual domain adaptation using subspace alignment," in *Proc. IEEE Int. Conf. Comput. Vis.*, 2013, pp. 2960–2967.
[26] C. Floudas and V. Visweswaran, "A global optimization algorithm (gop) for certain classes of nonconvex nlpsxi. theory," *Comput. Chem. Eng.*, vol. 14, no. 12, pp. 1397–1417, 1990.
[27] T. Gehrig and H. K. Ekenel, "A common framework for real-time emotion recognition and facial action unit detection," in *Proc. IEEE Conf. Comput. Vis. Pattern Recog. Workshop*, 2011, pp. 1–6.
[28] J. M. Girard, J. F. Cohn, L. A. Jeni, M. A. Sayette, and F. De la Torre, "Spontaneous facial expression in unscripted social interactions can be measured automatically," *Behavior Research Methods*, vol. 47, no. 4, pp. 1136-1147, 2014.
[29] D. A. Goldberg, M. B. Goldberg, M. D. Goldberg, and B. M. Goldberg, "Obtaining person-specific images in a public venue," U.S. Patent 7,561,723, 2009.
[30] J. Gorski, F. Pfeuffer, and K. Klamroth, "Biconvex sets and optimization with biconvex functions: A survey and extensions," *Math. Methods Operations Res.*, vol. 66, no. 3, pp. 373–407, 2007.
[31] A. Gretton, A. Smola, J. Huang, M. Schmittfull, K. Borgwardt, and B. Schölkopf, "Covariate shift by kernel mean matching," *Dataset Shift Mach. Learning*, vol. 3, no. 4, pp. 131–160, 2009.
[32] H. Gunes and M. Piccardi, "Affect recognition from face and body: Early fusion vs. late fusion," in *Proc. Int. Conf. Systems, Man Cybern.*, 2005, vol. 4, pp. 3437–3443.
[33] Y. Guo, G. Zhao, and M. Pietikäinen, "Dynamic facial expression recognition using longitudinal facial expression atlases," in *Proc. 10th Eur. Conf. Comput. Vis.*, 2012, pp. 631–644.
[34] L. A. Jeni, J. F. Cohn, and T. Kanade, "Dense 3d face alignment from 2d videos in real-time," in *Proc. IEEE Int. Conf. Autom. Face Gesture Recog.*, 2015.
[35] B. Jiang, M. F. Valstar, and M. Pantic, "Action unit detection using sparse appearance descriptors in space-time video volumes," in *Proc. Autom. Face Gesture Recog.*, 2011, pp. 314–321.
[36] T. Joachims, "Transductive inference for text classification using support vector machines," in *Proc. Int. Conf. Mach. Learn.*, 1999, pp. 200–209.
[37] T. Kanade, J. F. Cohn, and Y. Tian, "Comprehensive database for facial expression analysis," in *Proc. Autom. FaceGesture Recog.*, 2000, pp. 46–53.
[38] A. Kapoor and R. W. Picard, "Multimodal affect recognition in learning environments," in *Proc. ACM Int. Conf. Multimedia*, 2005, pp. 677-682.
[39] A. Khosla, T. Zhou, T. Malisiewicz, A. Efros, and A. Torralba, "Undoing the damage of dataset bias," in *Proc. 10th Eur. Conf. Comput. Vis.*, 2012, pp. 158-171.
[40] B. Kulis, K. Saenko, and T. Darrell, "What you saw is not what you get: Domain adaptation using asymmetric kernel transforms," in *Proc. IEEE Conf. Comput. Vis. Pattern Recog.*, 2011, pp. 1785–1792.

[41] G. Littlewort, J. Whitehill, T. Wu, I. Fasel, M. Frank, J. Movellan, and M. Bartlett, "The computer expression recognition toolbox (CERT)," in *Proc. IEEE Int. Conf. Autom. Face Gesture Recog.*, 2011, pp. 298–305.
[42] M. Liu, S. Li, S. Shan, and X. Chen, "AU-aware deep networks for facial expression recognition," in *Proc. IEEE Conf. Autom. Face Gesture Recog.*, 2013, pp. 1–6.
[43] B. D. Lucas and T. Kanade, "An iterative image registration technique with an application to stereo vision," in *Proc. Int. Joint Conf. Artif. Intell.*, 1981, pp. 674–679.
[44] P. Lucey, J. F. Cohn, T. Kanade, J. Saragih, Z. Ambadar, and I. Matthews, "The extended Cohn-Kanade dataset (CK+): A complete dataset for action unit and emotion-specified expression," in *Proc. IEEE Conf. Comput. Vis. Pattern Recog. Workshops*, 2010, pp. 94–101.
[45] S. Lucey, A. B. Ashraf, and J. Cohn, "Investigating spontaneous facial action recognition through AAM representations of the face," *Face Recog.*, pp. 275–286, 2007.
[46] A. Martinez and S. Du, "A model of the perception of facial expressions of emotion by humans: Research overview and perspectives," *J. Mach. Learning Res.*, vol. 13, pp. 1589–1608, 2012.
[47] I. Matthews and S. Baker, "Active appearance models revisited," *Int. J. Comput. Vis.*, vol. 60, no. 2, pp. 135–164, 2004.
[48] C. Orrite, A. Gañán, and G. Rogez, "Hog-based decision tree for facial expression classification," in *Proc. 4th Iberian Conf. Pattern Recog. Image Anal.*, 2009, pp. 176-183.
[49] M. Pantic and M. S. Bartlett, "Machine analysis of facial expressions," *Face Recog.*, pp. 377–416, 2007.
[50] J. Quionero-Candela, M. Sugiyama, A. Schwaighofer, and N. Lawrence, *Dataset Shift in Machine Learning*. Cambridge, MA, USA: MIT Press, 2009.
[51] B. Romera-Paredes, M. S. Aung, M. Pontil, N. Bianchi-Berthouze, A. de C Williams, and P. Watson, "Transfer learning to account for idiosyncrasy in face and body expressions," in *Proc. 10th IEEE Int. Conf. Workshops Automat. Face Gesture Recog.*, 2013, pp. 1–6.
[52] O. Rudovic, V. Pavlovic, and M. Pantic, "Kernel conditional ordinal random fields for temporal segmentation of facial action units," in *Proc. Eur. Conf. Comput. Vis. Workshop*, 2012, pp. 260–269.
[53] O. Rudovic, V. Pavlovic, and M. Pantic, "Context-sensitive dynamic ordinal regression for intensity estimation of facial action units," *IEEE Trans. Pattern Anal. Mach. Intell.*, vol. 37, no. 5, pp. 944–958, May 2015.
[54] K. Saenko, B. Kulis, M. Fritz, and T. Darrell, "Adapting visual category models to new domains," in *Proc. Eur. Conf. Comput. Vis.*, 2010, pp. 213-226.
[55] E. Sangineto, G. Zen, E. Ricci, and N. Sebe, "We are not all equal: Personalizing models for facial expression analysis with transductive parameter transfer," in *Proc. 22nd ACM Int. Conf. Multimedia*, 2014, pp. 357–366 .
[56] E. Sariyanidi, H. Gunes, and A. Cavallaro, "Automatic analysis of facial affect: A survey of registration, representation, and recognition," *IEEE Trans. Pattern Anal. Mach. Intell.*, vol. 37, no. 6, pp. 1113–1133, Jun. 2015.
[57] M. A. Sayette, K. G. Creswell, J. D. Dimoff, C. E. Fairbairn, J. F. Cohn, B. W. Heckman, T. R. Kirchner, J. M. Levine, and R. L. Moreland, "Alcohol and group formation a multimodal investigation of the effects of alcohol on emotion and social bonding," *Psychological Sci.*, vol. 23, no. 8, pp. 869–878, 2012.
[58] T. Senechal, V. Rapp, H. Salam, R. Seguier, K. Bailly, and L. Prevost, "Facial action recognition combining heterogeneous features via multikernel learning," *IEEE Trans. Syst., Man, Cybern., Part B: Cybern.*, vol. 42, no. 4, pp. 993–1005, Aug. 2012.
[59] L. Shang and K. Chan, "Nonparametric discriminant HMM and application to facial expression recognition," in *Proc. IEEE Conf. Comput. Vis. Pattern Recog.*, 2009, pp. 2090–2096.
[60] K. Sikka, T. Wu, J. Susskind, and M. Bartlett, "Exploring bag of words architectures in the facial expression domain," in *Proc. 12th Int. Conf. Comput. Vision*, 2012, pp. 250-259.
[61] T. Simon, M. H. Nguyen, F. De La Torre, and J. F. Cohn, "Action unit detection with segment-based SVMs," in *Proc. IEEE Conf. Comput. Vis. Pattern Recog.*, 2010, pp. 2737–2744.
[62] J. Sivic and A. Zisserman, "Video Google: A text retrieval approach to object matching in videos," in *Proc. IEEE Int. Conf. Comput. Vis.*, 2003, vol. 2, pp. 1470–1477.
[63] M. Sugiyama, M. Krauledat, and K. Müller, "Covariate shift adaptation by importance weighted cross validation," *J. Mach. Learning Res.*, vol. 8, pp. 985–1005, 2007.
[64] M. Sugiyama, S. Nakajima, H. Kashima, P. V. Buenau, and M. Kawanabe, "Direct importance estimation with model selection and its application to covariate shift adaptation," in *Proc. Adv. Neural Inf. Process. Syst.*, 2007, pp. 1433–1440.
[65] Y. Tong, W. Liao, and Q. Ji, "Facial action unit recognition by exploiting their dynamic and semantic relationships," *IEEE Trans. Pattern Anal. Mach. Intell.*, vol. 29, no. 10, pp. 1683–1699, Oct. 2007.
[66] A. Torralba and A. Efros, "Unbiased look at dataset bias," in *Proc. IEEE Conf. Comput. Vis. Pattern Recog.*, 2011, pp. 1521–1528.
[67] M. F. Valstar, M. Mehu, B. Jiang, M. Pantic, and K. Scherer, "Meta-analysis of the first facial expression recognition challenge," *IEEE Trans. Syst., Man, Cybern. Part B*, vol. 42, no. 4, pp. 966–979, Aug. 2012.
[68] M. F. Valstar and M. Pantic, "Fully automatic recognition of the temporal phases of facial actions," *IEEE Trans. Syst., Man, Cybern., Part B: Cybern.*, vol. 42, no. 1, pp. 28–43, Feb. 2012.
[69] T. Van Gestel, J. A. Suykens, B. Baesens, S. Viaene, J. Vanthienen, G. Dedene, B. De Moor, and J. Vandewalle, "Benchmarking least squares support vector machine classifiers," *Mach. Learning*, vol. 54, no. 1, pp. 5–32, 2004.
[70] Z. Wang, S. Wang, and Q. Ji, "Capturing complex spatio-temporal relations among facial muscles for facial expression recognition," in *Proc. IEEE Conf. Comput. Vis. Pattern Recog.*, 2013, pp. 3422–3429.
[71] R. E. Wendell and A. P. Hurter, "Minimization of a non-separable objective function subject to disjoint constraints," *Operations Res.*, vol. 24, no. 4, pp. 643–657, 1976.
[72] J. Whitehill, M. S. Bartlett, and J. R. Movellan, "Automatic facial expression recognition," *Soc. Emotions Nature Artifact*, vol. 88, 2013.
[73] T. Wu, M. S. Bartlett, and J. Movellan, "Facial expression recognition using Gabor motion energy filters," in *Proc. IEEE Conf. Comput. Vis. Pattern Recog. Workshop*, 2010, pp. 42–47.
[74] X. Xiong and F. De la Torre, "Supervised descent method and its applications to face alignment." in *Proc. IEEE Conf. Comput. Vis. Pattern Recog.*, 2013, pp. 532–539.
[75] M. Yamada, L. Sigal, and M. Raptis, "No bias left behind: Covariate shift adaptation for discriminative 3d pose estimation," in *Proc. 12th Eur. Conf. Comput. Vis.*, 2012, pp. 674–687.
[76] J. Yang, R. Yan, and A. Hauptmann, "Cross-domain video concept detection using adaptive SVMs," in *Proc. Int. Conf. Multimedia*, 2007, pp. 188–197.
[77] P. Yang, Q. Liu, and D. N. Metaxas, "Exploring facial expressions with compositional features," in *Proc. IEEE Conf. Comput. Vis. Pattern Recog.*, 2010, pp. 2638–2644.
[78] S. Yang, O. Rudovic, V. Pavlovic, and M. Pantic, "Personalized modeling of facial action unit intensity," in *Proc. Adv. Visual Comput.*, 2014, pp. 269–281.
[79] G. Zen, E. Sangineto, E. Ricci, and N. Sebe, "Unsupervised domain adaptation for personalized facial emotion recognition," in *Proc. Int. Conf. Multimodal Interaction*, 2014, pp. 128–135.
[80] J. Zeng, W.-S. Chu, F. De la Torre, J. F. Cohn, and Z. Xiong, "Confidence preserving machine for facial action unit detection," in *Proc. IEEE Int. Conf. Comput. Vis.*, 2015, pp. 3622–3630.
[81] H. Zhang, A. C. Berg, M. Maire, and J. Malik, "SVM-KNN: Discriminative nearest neighbor classification for visual category recognition," in *Proc. IEEE Conf. Comput. Vis. Pattern Recog.*, 2006, pp. 2126–2136.
[82] G. Zhao and M. Pietikainen, "Dynamic texture recognition using local binary patterns with an application to facial expressions," *IEEE Trans. Pattern Anal. Mach. Intell.*, vol. 29, no. 6, pp. 915–928, Jun. 2007.
[83] K. Zhao, W.-S. Chu, F. De la Torre, J. F. Cohn, and H. Zhang, "Joint patch and multi-label learning for facial action unit detection," in *Proc. IEEE Conf. Comput. Vis. Pattern Recog.*, 2015.
[84] L. Zhong, Q. Liu, P. Yang, B. Liu, J. Huang, and D. Metaxas, "Learning active facial patches for expression analysis," in *Proc. IEEE Conf. Comput. Vis. Pattern Recog.*, 2012, pp. 1499–1510.

[85] F. Zhou, F. De la Torre, and J. F. Cohn, "Unsupervised discovery of facial events," in *Proc. IEEE Conf. Comput. Vis. Pattern Recog.*, 2010, pp. 2574–2581.
[86] Y. Zhu, F. De la Torre, J. F. Cohn, and Y. J. Zhang, "Dynamic cascades with bidirectional bootstrapping for action unit detection in spontaneous facial behavior," *IEEE Trans. Affective Comput.*, vol. 2, no. 2, pp. 79–91, Apr.–Jun. 2011.

Wen-Sheng Chu received the BS and MS degrees in computer science from National Cheng Kung University, Tainan, Taiwan. He is currently working toward the PhD degree at the Robotics Institute, Carnegie Mellon University, Pittsburgh, PA, USA. His research interests lie in the development and use of machine learning techniques for computer vision problems. He is a student member of the IEEE and a member of the Phi Tau Phi Scholastic Honor Society.

Fernando De la Torre received the BSc degree in telecommunications, as well as the MSc and PhD degrees in electronic engineering from the La Salle School of Engineering at Ramon Llull University, Barcelona, Spain in 1994, 1996, and 2002, respectively. He is an associate research professor in the Robotics Institute at Carnegie Mellon University. His research interests are in the fields of computer vision and machine learning. Currently, he is directing the Component Analysis Laboratory (http://ca.cs.cmu.edu) and the Human Sensing Laboratory (http://humansensing.cs.cmu.edu) at Carnegie Mellon University. He has more than 150 publications in referred journals and conferences and is an associate editor at IEEE TPAMI. He has organized and co-organized several workshops and has given tutorials at international conferences on component analysis.

Jeffrey F. Cohn is a professor of psychology and psychiatry at the University of Pittsburgh and adjunct professor of computer science at the Robotics Institute at Carnegie Mellon University. He leads interdisciplinary and inter-institutional efforts to develop advanced methods of automatic analysis and synthesis of facial expression and prosody; and applies those tools to research in human emotion, social development, non-verbal communication, psychopathology, and biomedicine. He has served as a Co-Chair of the 2008 IEEE International Conference on Automatic Face and Gesture Recognition (FG2008), the *2009 International Conference on Affective Computing and Intelligent Interaction* (ACII2009), the *Steering Committee for IEEE International Conference on Automatic Face and Gesture Recognition*, and the *2014 International Conference on Multimodal Interfaces* (ACM 2014). He has co-edited special issues of the Journal of Image and Vision Computing and is a Co-Editor of IEEE Transactions in Affective Computing (TAC).